

# We are IntechOpen, the world's leading publisher of Open Access books Built by scientists, for scientists

6,900

Open access books available

186,000

International authors and editors

200M

Downloads

Our authors are among the

154

Countries delivered to

TOP 1%

most cited scientists

12.2%

Contributors from top 500 universities



WEB OF SCIENCE™

Selection of our books indexed in the Book Citation Index  
in Web of Science™ Core Collection (BKCI)

Interested in publishing with us?  
Contact [book.department@intechopen.com](mailto:book.department@intechopen.com)

Numbers displayed above are based on latest data collected.  
For more information visit [www.intechopen.com](http://www.intechopen.com)



# An Analytical Analysis of a Wind Power Generation System Including Synchronous Generator with Permanent Magnets, Active Rectifier and Voltage Source Inverter

Sergey A. Kharitonov, Member. IEEE  
Novosibirsk State Technical University  
Russia

## 1. Introduction

For the high-power Wind Power Installation (WPI) with a variable speed wind turbine the system of transformation of mechanical energy into electric energy of the alternating current, constructed under the scheme "the synchronous generator with constant magnets - the active rectifier - the voltage inverter" (fig. 1) is perspective. Then the system is called the Wind Power Generation System – WPGS.

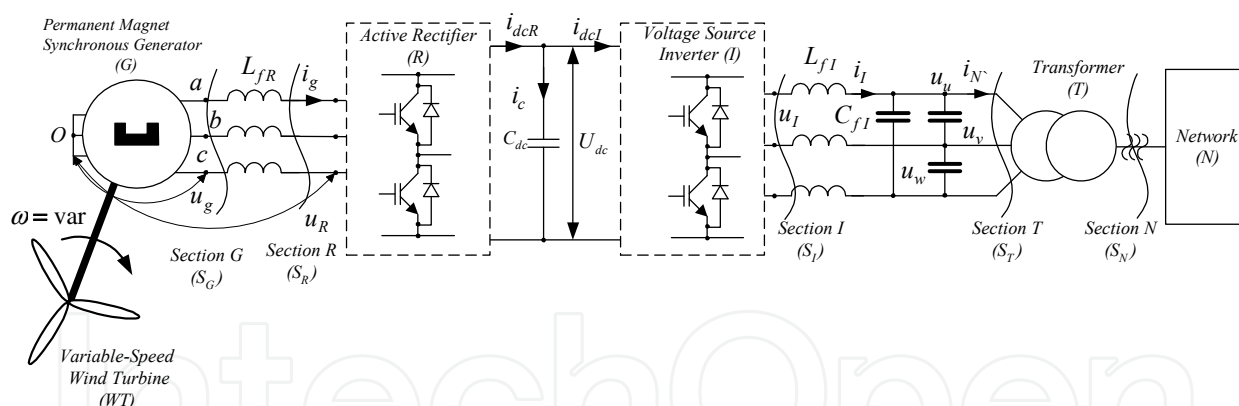


Fig. 1.

WPGS of this type implements the full set of options required from the generation for high-power WPI, namely this: a generating mode at work on the nonlinear, asymmetric and non-stationary loads, electric starter startup mode of the wind turbine, in-phase and parallel operation of an electric network and other WPI.

In this paper we attempt to identify the main energy characteristics of system in sections  $S_G, S_R, S_I, S_T, S_N$  (fig. 1) when working on high-power electric network. Processes in the active rectifier and the voltage inverter are well studied at a constant frequency and voltage of the generator. The peculiarity of this study is the consideration of factors that arise when working within the system to generate WPI with a variable rotation speed of the wind turbine. These factors include: changing the frequency and the voltage of the

Source: Wind Power, Book edited by: S. M. Muyeen,  
ISBN 978-953-7619-81-7, pp. 558, June 2010, INTECH, Croatia, downloaded from SCIYO.COM

synchronous generator (G), as well as dependence of the generated power on shaft speed of the wind turbine.

Presence in the system of the active rectifier (R) modifies the functional and energy potential of WPGS. The active rectifier with a PWM, which frequency is much higher than the voltage frequency of a synchronous generator (G), allows for a number of modes, significantly affecting the power consumption of G in the WPGS.

As a result of the conducted research where as an example it is accepted that the active rectifier and the inverter are based on the classical scheme of the two-level voltage inverter, the analytical description of WPGS system is obtained at a variable speed of rotation of the wind turbine, the basic expressions for currents, voltage and capacities of the synchronous generator, the voltage inverter are defined, algorithms of the management are offered by the active rectifier, and also the modular principle of construction of the voltage inverter and WPGS system as a whole are considered.

## 2. Basic assumptions. Mathematical model of the system.

For a generality of results of the analysis in the scheme elements which not always are obligatory are entered:

$L_{fR}$  - inductance of the cable connecting the generator and the active rectifier;

$T$  - the matching transformer;

$C_{fI}$  - capacity of the output filter, for the smoothing of pulsations on a transformer input.

The active rectifier and the voltage inverter are controlled by a high-frequency PWM, and their frequencies  $\omega_{cR}$  and  $\omega_{cI}$ , correspondingly, are significantly higher than frequencies of the fundamental harmonic voltage of synchronous generator ( $\omega$ ) and the electric voltage network ( $\Omega$ ). The multiplicities of frequencies are constant, i.e.  $\omega_{cR}/\omega = a_R = const$  and  $\omega_{cI}/\Omega = a_I = const$ .

The electrical network has a capacity much bigger than the power of WPI.

Let's assume also that the synchronous generator does not contain soothing contours and its magnetic system is linear.

The generating mode is a subject to consideration. In this case, the active rectifier (R) entrusted with the tasks of forming a given voltage in the DC link  $U_{dc}$  and reactive power control on the frequency  $\omega$  in sections  $S_G$  and  $S_R$ , while the voltage inverter (I) is tasked to ensure the specified quality and quantity of the generated current in the electric network.

Let's consider that the capacity  $C_{dc}$  in a DC link is big, the voltage regulator  $U_{dc}$  in a control system works with the maximum speed and is non-static then in the established mode it is possible to accept that  $U_{dc} = const$ . In this case in sections  $S_G, S_R$  it is possible to consider the electromagnetic processes irrespective of processes in sections  $S_I, S_N$  and  $S_T$ .

It is convenient to study WPGS in the rotating coordinate systems. In this case in section  $S_G$  the coordinate system rotates synchronously with the frequency of the generator voltage ( $\omega$ ), and in sections  $S_I, S_N$  respectively, with the frequency of the mains voltage ( $\Omega$ ).

Taking into account the accepted assumptions *the mathematical model of SG* in rotating system of co-ordinates, under condition of axis orientation d on a longitudinal axis of the synchronous generator will look like:

$$\mathbf{u}_R = -r_\Sigma \mathbf{i}_G - \frac{d}{dt} \boldsymbol{\psi}_\Sigma - \boldsymbol{\omega} \boldsymbol{\psi}_\Sigma, \quad \boldsymbol{\psi}_\Sigma = \mathbf{L}_\Sigma \mathbf{i}_G - \boldsymbol{\psi}_0 \quad (1)$$

where:  $\boldsymbol{\psi}_\Sigma = [\Psi_{\Sigma d} \quad \Psi_{\Sigma q}]^t$ ,  $\Psi_{\Sigma d} = \Psi_d + L_{fR} i_{Gd}$ ,  $\Psi_{\Sigma q} = \Psi_q + L_{fR} i_{Gq}$ ,  $\Psi_d, \Psi_q$  - the magnetic flux of generator in the longitudinal and transverse axes,  $\mathbf{u}_R = [u_{Rd} \quad u_{Rq}]^t$ ,  $\mathbf{i}_g = [i_{Gd} \quad i_{Gq}]^t$  - vectors of the active rectifier voltages and currents of the generator;  $\boldsymbol{\psi}_0 = [\Psi_0 \quad 0]^t$ ,  $\Psi_0 = const$  - the magnetic flux created by permanent magnets;  $r_\Sigma = diag\{r_\Sigma, r_\Sigma\}$ ,  $r_\Sigma = r_s + r_{LFR}$ ,  $r_s, r_{LFR}$  - the active resistances of stator phase windings of the generator and cable connecting the generator and active rectifier;  $\mathbf{L}_\Sigma = diag\{L_{\Sigma d}, L_{\Sigma q}\}$ ,  $L_{\Sigma d} = L_d + L_{fR}$ ,  $L_{\Sigma q} = L_q + L_{fR}$ ,  $L_d, L_q$  - inductance of the generator in the longitudinal and transverse axes;  $\boldsymbol{\omega} = \begin{bmatrix} 0 & -\omega \\ \omega & 0 \end{bmatrix}$ ,  $\omega$  - circular frequency of the electromotive force (EMF) of SG ( $\omega = var$ ).

Selecting the generator currents as variables, after simple transformations, we obtain from equation (1):

$$\mathbf{u}_R = -r_\Sigma \mathbf{i}_G - \mathbf{L}_\Sigma \frac{d}{dt} \mathbf{i}_G - \boldsymbol{\omega} \mathbf{L}_\Sigma \mathbf{i}_G + \mathbf{e} \quad \mathbf{e} = [0 \quad E_0]^t, \quad (2)$$

here  $E_0 = \boldsymbol{\omega} \boldsymbol{\psi}_0$  - EMF-load of the generator ( $E_0 = var$ ).

Neglecting the active resistance it is possible to write down parity (2) in the scalar form

$$\begin{aligned} u_{Rd} &= -i_{Gd} \cdot r_s - L_{d\Sigma} \frac{di_{Gd}}{dt} + \omega L_{q\Sigma} i_{Gq} \approx -L_{d\Sigma} \frac{di_{Gd}}{dt} + \omega L_{q\Sigma} i_{Gq}, \\ u_{Rq} &= -i_{Gq} \cdot r_s - L_{q\Sigma} \frac{di_{Gq}}{dt} - \omega L_{d\Sigma} i_{Gd} + E_0 \approx -L_{q\Sigma} \frac{di_{Gq}}{dt} - \omega L_{d\Sigma} i_{Gd} + E_0 \end{aligned} \quad (3)$$

In any section S active ( $P_S$ ), reactive ( $Q_S$ ) and apparent ( $S_S$ ) powers will be defined by means of the following parities:

$$P_S = \frac{3}{2}(\mathbf{u}, \mathbf{i}) = \frac{3}{2}(u_d i_d + u_q i_q), \quad Q_S = \frac{3}{2}[\mathbf{u}, \mathbf{i}] = \frac{3}{2}(u_d i_q - u_q i_d), \quad S_S = [P_S^2 + Q_S^2]^{\frac{1}{2}}. \quad (4)$$

The mathematical description of the active rectifier and the inverter will be obtained by means of switching functions. We will consider that transistors and diodes are ideal keys. R and I are realized on base of the voltage inverter schematically presented in fig. 2.

The phase voltage on alternating current clips is defined by means of parity:

$$u_m = U_{dc} \left( 2F_m - \sum_{\substack{k=1 \\ k \neq m}}^3 F_k \right) / 3; \quad m = 1, 2, 3, \quad (5)$$

where  $F_m$  - the switching functions of transistors  $VT_m$  of the inverter which are defined by

means of a following parity  $F_m = \begin{cases} 1, & VT_m - \text{is switched on;} \\ 0, & VT_m - \text{is switched off.} \end{cases}$

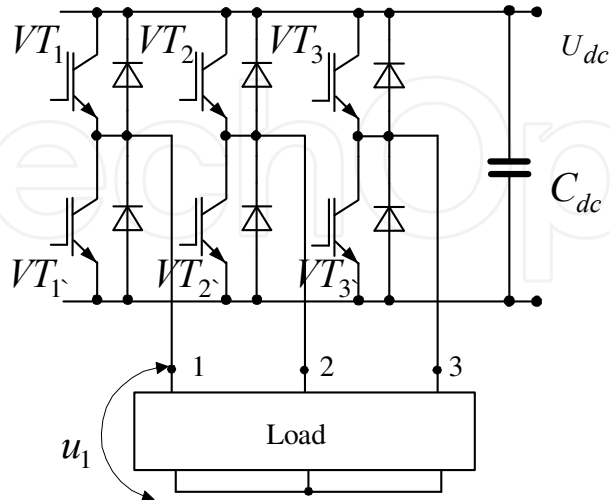


Fig. 2.

They also can be defined by means of a series:

$$F_m = M \sin \theta_m / 2 + \sum_{j=1}^{\infty} F_{msj} \sin(j \cdot a_k \vartheta) + F_{mcj} \cos(j \cdot a_k \vartheta);$$

$$F_{msj} = \frac{(-1)^j}{j\pi} [(-1)^j - \cos(j\pi \cdot M \sin \theta_m)]; \quad F_{mcj} = \frac{(-1)^j}{j\pi} \sin(j\pi \cdot M \sin \theta_m);$$

$$M = \begin{cases} u_c / u_{sc} & \text{SPWM;} \\ 2u_c / \sqrt{3}u_{sc} & \text{SVPWM;} \end{cases} \quad M_{\max} = \begin{cases} 1 & \text{SPWM;} \\ 2/\sqrt{3} & \text{SVPWM;} \end{cases} \quad \theta_m = \vartheta - (m-1) \frac{2\pi}{3} + \phi_c;$$

where:  $\vartheta = \omega t$ ,  $a_k = \omega_c / \omega$ ,  $\omega_c$ ,  $\omega$  - the cyclic frequencies of PWM and an of operating signal, accordingly,  $M$ ,  $M_{\max}$  - the depth (index) of modulation and its maximum value,  $u_c$  - amplitude of the control input wave,  $u_{sc}$  - the amplitude of saw tooth carrier wave,  $\phi_c$  - the phase of the control input wave, is defined by the chosen algorithm of control. After a number of transformations we will obtain for SPWM

$$u_m = U_{dc} M \sin(\theta_m) / 2 + \frac{U_{dc}}{\pi} \sum_{\substack{p=-\infty \\ p \neq 0}}^{\infty} \sum_{k=-\infty}^{\infty} (-1)^{p+3k} / p \cdot J_{3k+1}(p\pi M) \cdot \sin[a_k p \vartheta + (3k+1)\theta_m];^1 \quad (6)$$

where  $J_{3k+1}(\dots)$  - Bessel functions of the first kind of an order  $3k+1$ .

Obviously, expression for the fundamental component will look like:

$$u_{m(1)} = U_{dc} M \sin(\theta_m) / 2.$$

<sup>1</sup> In this parity and further the high-frequency harmonics are defined for SPWM.

If we introduce the operator of rotation  $a = \exp(i \cdot 2\pi/3)$ ,  $i = \sqrt{-1}$ ,  $u_m, m = 1, 2, 3$  the three voltages can be written in the orthogonal coordinate system:

$$u_{\alpha\beta} = u_\alpha + i \cdot u_\beta = \frac{2}{3}(u_1 + a \cdot u_2 + a^2 \cdot u_3).$$

Using parity (6), we will obtain:

$$u_\alpha = \frac{U_{dc}}{2} M \sin(\theta_1) + \frac{U_{dc}}{\pi} \sum_{\substack{p=-\infty \\ p \neq 0}}^{\infty} \sum_{k=-\infty}^{\infty} \frac{(-1)^{p+3k}}{p} J_{3k+1}(p\pi \cdot M) \sin[ap\vartheta + (3k+1)\theta_1]; \quad (7)$$

$$u_\beta = -\frac{U_{dc}}{2} M \cos(\theta_1) - \frac{U_{dc}}{\pi} \sum_{\substack{p=-\infty \\ p \neq 0}}^{\infty} \sum_{k=-\infty}^{\infty} \frac{(-1)^{p+3k}}{p} J_{3k+1}(p\pi \cdot M) \cos[ap\vartheta + (3k+1)\theta_1]. \quad (8)$$

We will determine the current in a direct current link ( $i_{dc}$ ) by means of parity:

$$i_{dc} = \sum_{m=1}^3 i_{gm} F_m, \text{ where } i_{gm} - \text{the instant value of phase currents of the generator. The average}$$

value of current  $i_{dc}$  from the condition of equality of the active power in AC and DC circuits of inverter is:  $I_{dco} = 3MI_{(1)} \cos\varphi/4$ , here  $\varphi$  - an angle shift between the fundamental harmonic of phase voltage and an inverter current,  $I_{(1)}$  - the amplitude of inverter current,  $I_{dco}$  - the mean value of a current in a DC link.

*In the analysis of electromagnetic processes in sections  $S_I, S_T, S_N$  we will assume that  $\omega_{kl} \gg \Omega$ . In a first approximation it allows to neglect the effect of capacitors  $C_{fl}$ . When considering the transformer ( $T$ ), we assume that its magnetic system is unsaturated, active losses and the magnetization current are zero and its influence on the processes we take into account with the total leakage inductance ( $L_{\sigma T}$ ) and transformation factor ( $k_T$ ):  $k_T = w_1/w_2$ ;  $L_{\sigma T} = L_{\sigma 1T} + L_{\sigma 2T} = L_{\sigma 1T} + L_{\sigma 2T} \cdot k_T^2$ ; where  $w_1, w_2$ , - the number of turns of primary and secondary windings of the transformer,  $L_{\sigma 1T}, L_{\sigma 2T}$  - the leakage inductance of primary and secondary windings, respectively.*

We will express the voltage of an electric network through the voltage on a primary winding of the transformer using the relation:  $u_{N'} = u_N \cdot k_T$ . The equivalent inductance in the output circuit of inverter:  $L_I = L_f + L_{\sigma T}$ .

Taking into account the accepted assumptions WPGS can be presented in the form of two equivalent circuits, for example, in phase coordinates fig. 3 and fig. 4.

In these figures dependent sources of voltage which reflect the voltages R and I in alternating current clips are presented in the form of rhombs. These voltages are defined by relation (5).

### 3. Basic energy indicators in the chain of "synchronous generator - active rectifier"

The power quality parameters of electromagnetic processes in WPGS determine the technical efficiency of converting mechanical energy of a shaft rotating with a variable speed

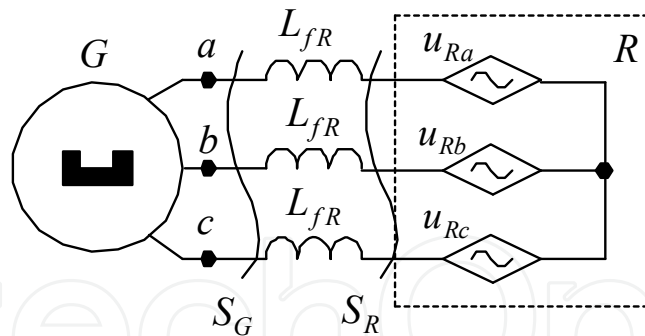


Fig. 3.

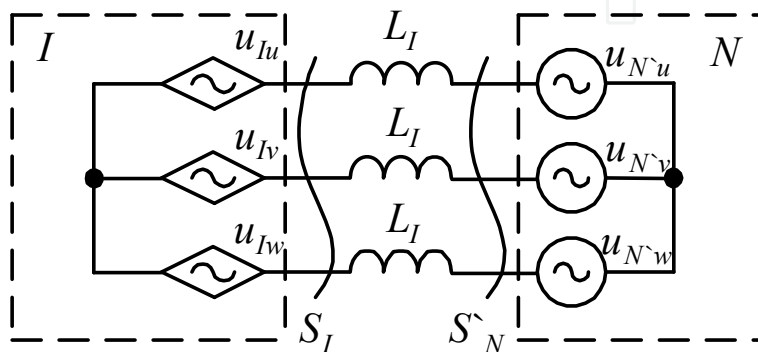


Fig. 4.

wind turbine into electrical energy by means of a synchronous generator and the voltage inverter, and the degree of influence of WPGS on the electric network through quality indicators of the electricity generated.

The basic indicators include: efficiency, power factor, and factors of harmonics and distortions of currents and voltages. For calculation of these indicators the definition of the operating values of currents and voltages in system elements is necessary, therefore they also are indirect power indicators.

For generality of the results, we introduce the relative units, as a basic value we choose the following:

$$U_{dc} = \sqrt{3}U_{N^*}; \quad E_{\delta} = \frac{U_{dc}}{\sqrt{3}} = U_{N^*}; \quad \omega_{\delta} = \frac{E_{\delta}}{\Psi_o}; \quad X_{\delta} = \omega_{\delta}(L_f + L_d) = \omega_{\delta}L_d(1+q);$$

$$I_{\delta} = I_{\kappa 3} = \frac{E_{\delta}}{X_{\delta}}; \quad S_{\delta} = \frac{3}{2} \cdot E_{\delta}I_{\delta}; \quad \omega^* = \frac{\omega}{\omega_{\delta}}, \quad E_o^* = \frac{E_o}{E_{\delta}} = \omega^*, \quad u^* = \frac{u}{E_{\delta}}, \quad i^* = \frac{i}{I_{\delta}}, \quad a_R = \frac{\omega_{cR}}{\omega}, \quad (9)$$

where  $U_{N^*}$  - the amplitude value of voltage of electrical network, referred to the primary winding,  $\omega_{cR}$  the cyclic frequency PWM of an active rectifier.

Denote:

$$q = \frac{L_f}{L_d}; \quad k_x = \frac{L_{aq}}{L_{ad}}; \quad \sigma = \frac{L_{\sigma}}{L_{ad}}; \quad k_L = \frac{L_q}{L_d} = \frac{\sigma + k_x}{\sigma + 1}. \quad (10)$$

Taking into account (9) and (10) we obtain:

$$X_{fR}^* = \frac{X_{fR}}{X_{\bar{\sigma}}} = \frac{\omega^* q}{1+q}, X_d^* = \frac{X_d}{X_{\bar{\sigma}}} = \frac{\omega^*}{1+q}, X_q^* = \frac{X_q}{X_{\bar{\sigma}}} = \frac{\omega^*}{1+q} k_L,$$

$$X_{d\Sigma}^* = X_d^* + X_{fR}^* = \omega^*, X_{q\Sigma}^* = X_q^* + X_{fR}^* = \omega^* \frac{k_L + q}{1+q}.$$

Considering relative units and the entered designations of the equation (3) will become:

$$u_{Rd}^* = -X_{d\Sigma}^* \frac{di_{Gd}^*}{d\vartheta} + X_{q\Sigma}^* i_{Gq}^* = -\omega^* \frac{di_{Gd}^*}{d\vartheta} + \omega^* \frac{k_L + q}{1+q} \cdot i_{Gq}^*;$$

$$u_{Rq}^* = -X_{q\Sigma}^* \frac{di_{Gq}^*}{d\vartheta} - X_{d\Sigma}^* i_{Gd}^* + \omega^* = -\omega^* \frac{k_L + q}{1+q} \cdot \frac{di_{Gq}^*}{d\vartheta} - \omega^* i_{Gd}^* + \omega^*,$$
(11)

where  $\vartheta = \omega t$ .

Accordingly, we will define the power for the basic harmonics in sections  $S_G$  also  $S_R$  by means of expressions:

$$\begin{cases} P_{SGo}^* = P_{SRo}^* = P_{SNo}^* = \omega^* i_{gqo}^*, \\ Q_{SGo}^* = u_{Gdo}^* i_{Gqo}^* - u_{Gqo}^* i_{Gdo}^*; \quad Q_{SRo}^* = u_{Rdo}^* i_{Gqo}^* - u_{Rqo}^* i_{Gdo}^*; \\ S_{SGo}^* = [(P_{SNo}^*)^2 + (Q_{SGo}^*)^2]^{\frac{1}{2}}; \quad S_{SRo}^* = [(P_{SNo}^*)^2 + (Q_{SRo}^*)^2]^{\frac{1}{2}}; \end{cases}$$
(12)

here it is considered that at the accepted assumptions the active power is identical and equal in all sections to the power generated in an electric network ( $P_{SNo}^*$ ).

Taking into account the higher harmonics value of active power will not change, and to calculate inactive and a total power it is necessary to apply the following relations:

$$P_{SG}^* = P_{SR}^* = P_{SGo}^*; \quad S_{SG}^* = U_{G,rms}^* I_{G,rms}^*; \quad S_{SR}^* = U_{R,rms}^* I_{G,rms}^*;$$

$$Q_{SG}^* = \sqrt{(S_{SG}^*)^2 - (P_{SG}^*)^2}; \quad Q_{SR}^* = \sqrt{(S_{SR}^*)^2 - (P_{SR}^*)^2}$$

We will define the power factor in sections  $S_R$  also  $S_R$  by means of parities:

$$\chi_G = P_{SG}^* / S_{SG}^* = v_{iG} v_{uG} \cos \varphi_{SG}; \quad \chi_R = P_{SR}^* / S_{SR}^* = v_{iG} v_{uR} \cos \varphi_{SR},$$
(13)

where:  $v_{iSG} = I_{G(1),rms}^* / I_{G,rms}^*$ ,  $v_{uSG} = U_{G(1),rms}^* / U_{G,rms}^*$ ,  $v_{uSR} = U_{R(1),rms}^* / U_{R,rms}^*$ ,  $v_{iS}$ ,  $v_{uS}$ ,  $\varphi_S$  - a fundamental factors of current and voltage, and also a shift angle between the basic harmonics of current and voltage accordingly in sections  $S_G$  and  $S_R$ ,  $I_{G(1),rms}^*$ ,  $I_{G,rms}^*$ ,  $U_{G(1),rms}^*$ ,  $U_{G,rms}^*$ ,  $U_{R(1),rms}^*$ ,  $U_{R,rms}^*$  - root-mean-square - RMS of the basic harmonics and full values of a current and a voltage in corresponding sections.

Assuming that the EMF-load of generator ( $e_{Gm}^*$ ) and the control voltage of an active rectifier ( $u_{Rcm}^*$ ) varies according to the law:

$$e_{Gm}^* = \omega^* \cos \left[ \vartheta - (m-1) \frac{2\pi}{3} \right]; u_{Rcm}^* = M \sin(\theta_m);$$

$$\theta_m = \vartheta - (m-1) \frac{2\pi}{3} + \frac{\pi}{2} - \phi_{Rc}; \vartheta = \omega t; m = 1, 2, 3 (a, b, c);$$

and taking into account the relation (7, 8), we obtain expressions for the quantities  $u_{Rd}^*$  and  $u_{Rq}^*$ :  $u_{Rdq}^* = u_{Rd} + i \cdot u_{Rq} = u_{R\alpha\beta}^* \exp[-i \cdot \gamma(\vartheta)]$ , where  $\gamma(\vartheta) = \vartheta - \pi/2$ .

At the analysis in « $d q$ » co-ordinates it is convenient to present the three control input waves of the active rectifier in the form of two orthogonal projections on  $d$  and  $q$  axes, then  $M_d = M \sin \phi_{Rc}$ ;  $M_q = M \cos \phi_{Rc}$ , it is obvious that  $M = \sqrt{M_d^2 + M_q^2}$ .

After the transformations we will obtain an expression for voltage of the active rectifier in « $d q$ » co-ordinates:

$$u_{Rd}^* = u_{Rdo}^* + \Delta u_{Rd}^*; \quad u_{Rq}^* = u_{Rqo}^* + \Delta u_{Rq}^*; \quad u_{Rdo}^* = \sqrt{3} M_d / 2; \quad u_{Rqo}^* = \sqrt{3} M_q / 2;$$

$$\Delta u_{Rd}^* = \frac{\sqrt{3}}{\pi} \sum_{p \neq 0} \sum_{k=-\infty}^{\infty} \frac{(-1)^{p+k}}{p} \cdot J_{3k+1}(p\pi \cdot M) \cos[a_R p \vartheta + 3k \vartheta + (3k+1)(\pi/2 - \phi_{Rc})]; \quad (14)$$

$$\Delta u_{Rq}^* = \frac{\sqrt{3}}{\pi} \sum_{p \neq 0} \sum_{k=-\infty}^{\infty} \frac{(-1)^{p+k}}{p} \cdot J_{3k+1}(p\pi \cdot M) \sin[a_R p \vartheta + 3k \vartheta + (3k+1)(\pi/2 - \phi_{Rc})],$$

here  $u_{Rdo}^*, u_{Rqo}^*$  - the orthogonal components in  $d$  and  $q$  coordinates of the basic harmonic of voltage of the active rectifier;  $\Delta u_{Rd}^*, \Delta u_{Rq}^*$  - the orthogonal components in  $d$  and  $q$  coordinates of the high-frequency harmonics of voltage of the active rectifier.

In the steady operating mode for a particular value of generator voltage frequency ( $\omega^*$ ) with the help of relations (11) and (14) we can determine an analytical expression for the generator currents. To do this in (14) we will allocate sinus and cosine components ( $U_{Rds pk}^*, U_{Rdc pk}^*, U_{Rqs pk}^*, U_{Rqc pk}^*$ ) of the harmonics with frequencies  $\nu_{pk} = a_R p \omega + 3k \omega$ :

$$U_{Rds pk}^* = -g_{kp} \sin[(3k+1)(\pi/2 - \phi_{Rc})]; \quad U_{Rqs pk}^* = g_{kp} \cos[(3k+1)(\pi/2 - \phi_{Rc})];$$

$$U_{Rdc pk}^* = g_{kp} \cos[(3k+1)(\pi/2 - \phi_{Rc})]; \quad U_{Rqc pk}^* = g_{kp} \sin[(3k+1)(\pi/2 - \phi_{Rc})], \quad (15)$$

here  $g_{kp} = \frac{\sqrt{3}}{\pi} \frac{(-1)^{p+k}}{p} \cdot J_{3k+1}(p\pi \cdot M)$ .

The equation for the generator current can be represented as a sum of components from the fundamental ( $i_{Gdo}^*, i_{Gqo}^*$ ) and the high-frequency ( $\Delta i_{Gd}^*, \Delta i_{Gq}^*$ ) harmonics

$$i_{Gd}^* = i_{Gdo}^* + \Delta i_{Gd}^*; \quad i_{Gq}^* = i_{Gqo}^* + \Delta i_{Gq}^*.$$

Then, using equations (11) and (15), we obtain

$$i_{Gq0}^* = \frac{u_{Rd0}^*}{X_{q\Sigma}^*} = \frac{1+q}{\omega^*(k_L+q)} \cdot u_{Rd0}^* = \frac{\sqrt{3}}{2} \frac{1+q}{\omega^*(k_L+q)} M_d, \quad i_{Gd0}^* = 1 - \frac{u_{Rq0}^*}{\omega^*} = 1 - \frac{\sqrt{3}}{2} \frac{1}{\omega^*} M_q.$$

$$\begin{aligned} \Delta i_{Gd}^*(\vartheta) &= \sum_{\substack{p=-\infty \\ p \neq 0}}^{\infty} \sum_{k=-\infty}^{\infty} \left[ I_{Gds\,pk}^* \sin(a_R p + 3k)\vartheta + I_{Gdc\,pk}^* \cos(a_R p + 3k)\vartheta \right]; \\ \Delta i_{Gq}^*(\vartheta) &= \sum_{\substack{p=-\infty \\ p \neq 0}}^{\infty} \sum_{k=-\infty}^{\infty} \left[ I_{Gqs\,pk}^* \sin(a_R p + 3k)\vartheta + I_{Gqc\,pk}^* \cos(a_R p + 3k)\vartheta \right]; \end{aligned} \tag{16}$$

where:

$$I_{Gds\,pk}^* = g d_{kp} [U_{Rqs\,pk} - U_{Rdc\,pk}(a_R p + 3k)]; \quad I_{Gdc\,pk}^* = g d_{kp} [U_{Rqc\,pk} - U_{Rds\,pk}(a_R p + 3k)];$$

$$I_{Gqs\,pk}^* = g q_{kp} [U_{Rds\,pk} + U_{Rqc\,pk}(a_R p + 3k)]; \quad I_{Gqc\,pk}^* = g q_{kp} [U_{Rdc\,pk} + U_{Rqs\,pk}(a_R p + 3k)],$$

here  $g d_{kp} = 1/[(a_R p + 3k)^2 - 1]X_{d\Sigma}$ ,  $g q_{kp} = -1/[(a_R p + 3k)^2 - 1]X_{q\Sigma}$ .

Voltage of the synchronous generator is defined as follows:

$$u_{Gd}^* = \Delta u_{Gd}^* + u_{Gd0}^*; \quad u_{Gq}^* = \Delta u_{Gq}^* + u_{Gq0}^*$$

$$\begin{aligned} u_{Gd0}^* &= u_{Rd0}^* - X_{Rf}^* i_{Gq0}^* = \frac{\sqrt{3}}{2} \frac{k_L}{k_L + q} M \sin(\varphi_{RC}); \\ u_{Gq0}^* &= u_{Rq0}^* + X_{Rf}^* i_{Gd0}^* = \frac{1}{1+q} \left[ \omega^* q + \frac{\sqrt{3}}{2} M \cos(\varphi_{RC}) \right]; \end{aligned} \tag{17}$$

$$\Delta u_{Gd}^* = \Delta u_{Rd}^* + X_{Rf}^* \frac{d i_{Gd}^*}{d\vartheta} - X_{Rf}^* \Delta i_{Gq}^*; \quad \Delta u_{Gq}^* = \Delta u_{Rq}^* + X_{Rf}^* \frac{d \Delta i_{Gq}^*}{d\vartheta} + X_{Rf}^* \Delta i_{Gd}^*.$$

here  $u_{Gd0}^*, u_{Gq0}^*$  - the orthogonal components in the  $d$  and  $q$  coordinates of the fundamental harmonic of generator voltage,  $\Delta u_{Gd}^*, \Delta u_{Gq}^*$  - the orthogonal components in the  $d$  and  $q$  coordinates of the high-frequency harmonics of generator voltage.

From (16a) and (17) can easily be obtained the following useful relations:

$$u_{Gd0}^* = k_L u_{Rd0}^* / (k_L + q), \quad u_{Gq0}^* = (u_{Rq0}^* + q\omega^*) / (1 + q). \tag{18}$$

RMS of the active rectifier voltage ( $U_{R,rms}$ ) and its fundamental factor can be determined if we use the following properties of switching functions  $F_m$  [1]:

$$\frac{1}{2\pi} \cdot \int_0^{2\pi} (F_j)^2 d\vartheta = \frac{1}{2}; \quad \frac{1}{2\pi} \cdot \int_0^{2\pi} F_j \cdot F_i d\vartheta \approx \frac{1}{2} \cdot (1 - 0.5M); \quad i, j = 1, 2, 3; (i \approx j).$$

Then:

$$U_{R,rms}^* = \sqrt{M/2}; \quad v_{uR} = \frac{U_{R(1),rms}}{U_{R,rms}} = \sqrt{3M/2}.$$

We define RMS of the generator current through the equation:

$$I_{G,rms}^* = \sqrt{(i_{Gdo}^*)^2 + (i_{Gqo}^*)^2 + (\Delta I_G^*)^2} / \sqrt{2}, \quad (19)$$

where

$$\Delta I_G^* \approx \left( \frac{\sqrt{6}}{\pi \cdot \omega^*} \right) \cdot \left( J_1(\pi \cdot M)^2 \frac{a_R^2 + 1}{(a_R + 1)^2 (a_R - 1)^2} \right)^{\frac{1}{2}}. \quad (19a)$$

Then the fundamental factor of the generator current can be estimated using the relation:

$$v_{iG} = \sqrt{\frac{(i_{Gdo}^*)^2 + (i_{Gqo}^*)^2}{(i_{Gdo}^*)^2 + (i_{Gqo}^*)^2 + (\Delta I_{Gdq}^*)^2}}.$$

We will determine RMS of the generator voltage considering that,  $k_L \rightarrow 1$ , then:

$$U_{G,rms}^* = \frac{1}{\sqrt{2}} \sqrt{(\omega^* \cos \theta)^2 + \frac{1}{(1+q)^2} \left[ M - \left( \frac{\sqrt{3}}{2} M \cos \phi_c \right)^2 \right]},$$

where  $\theta$  - the angle between the main harmonics of the EMF and the generator voltage. In accordance with the vector diagram (fig. 5)  $\theta$  is given by:  $\theta = \arctg u_{Gdo}^* / u_{Gqo}^*$ .

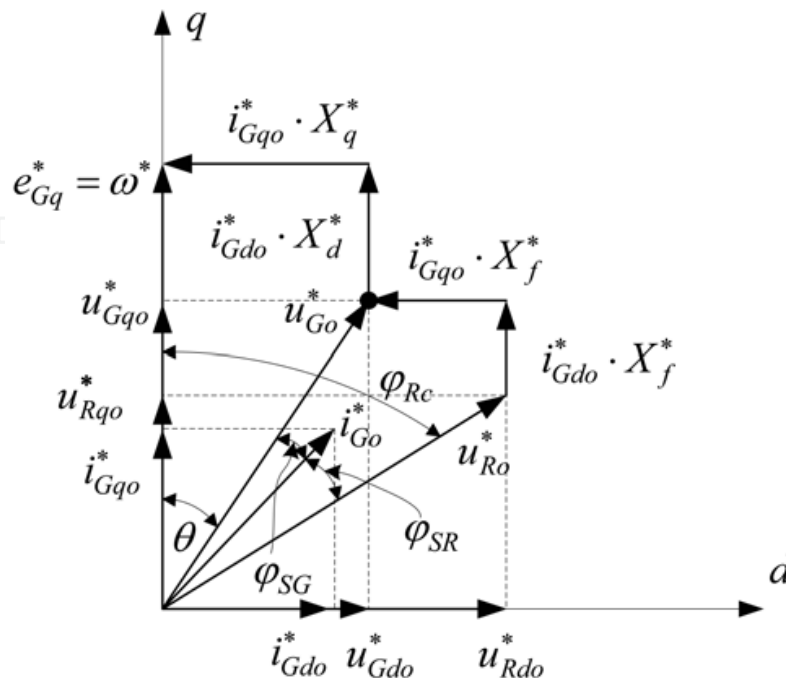


Fig. 5.

In fig.6 as an illustration of the possibilities suggested by the mathematical model of the system the calculated dependences of some power indicators as change of frequency of rotation of the wind turbine for a mode  $i_{Gdo}^* = 0$ , i.e. when a phase of a current and EMF of the generator coincide are presented. In this case the active filter increases the voltage  $u_{Ro}^* > e_G^*$ .

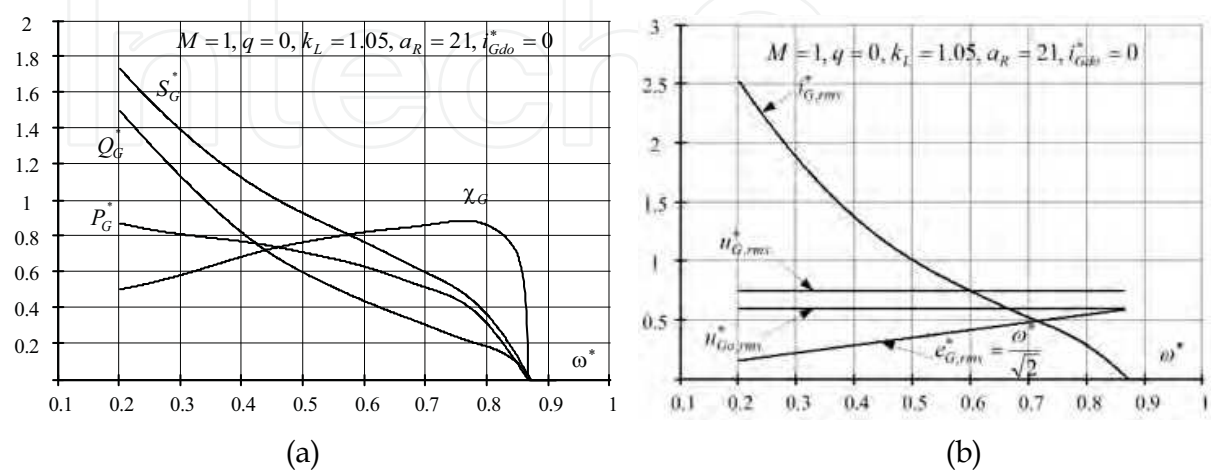


Fig. 6.

Dependence of the fundamental factor of the generator current on the modulation depth and speed of the wind turbine for different multiplicities of frequencies is presented in fig. 7. It follows from these graphs, in engineering calculations, and when  $a_R > 15 \div 20$  and  $\omega^* = 0.4 \div 0.8$  you can take  $v_{iR} \approx 1$ . This means that the active power generated by the system is determined by the fundamental harmonics of current and voltage.

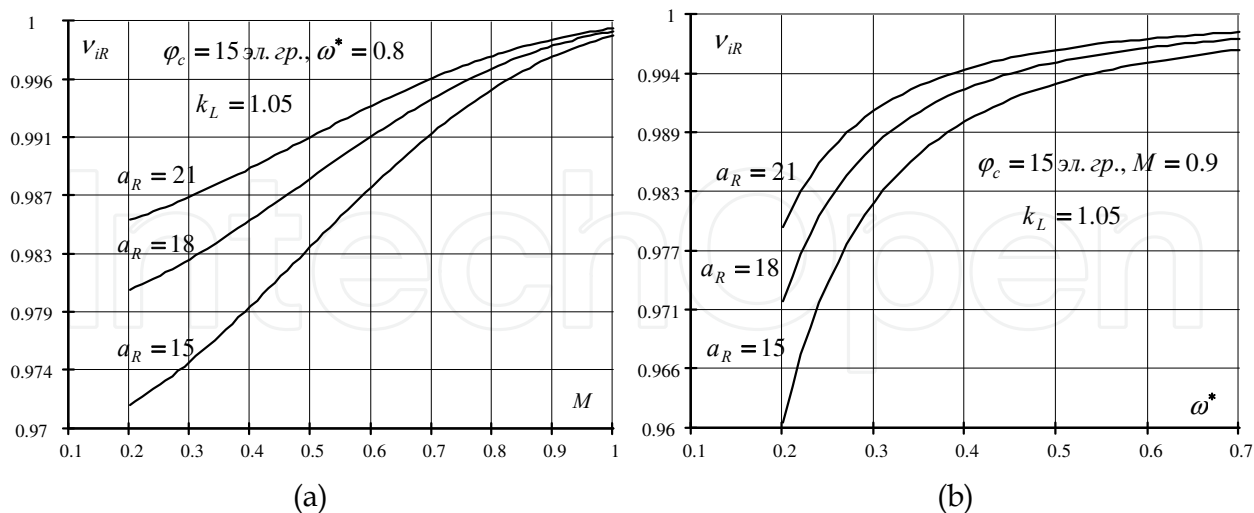


Fig. 7.

Let's consider the character of change of generated power, and also currents and voltages using (11), (12) and (16a). For the real synchronous generators it is characteristic  $L_d \approx L_q$ , i.e.  $k_L \rightarrow 1$ ; besides this, usually, the inequality  $L_f < L_d$  takes place, so  $q < 1$ .

For WPI with a variable speed wind turbine the generated active power ( $P_{WT0}^*$ ) in the working range ( $\omega^* \in \{\omega_{WT\min}^*, \omega_{WT\max}^*\}$ ) is determined by the speed of the wind and can be calculated for the known characteristics of the turbine using the relation:

$$P_{WT0}^* = \gamma \cdot (\omega^*)^3. \quad (20)$$

where  $\gamma$  - a constant coefficient determined by the design of wind turbine;  $\{\omega_{WT\min}^*, \omega_{WT\max}^*\}$  - the working range, also characterized by the value  $D_{WT} = \omega_{WT\max}^* / \omega_{WT\min}^*$ ;  $\omega_{WT\min}^*, \omega_{WT\max}^*$  - the minimum and maximum operating speed of WT, respectively.

Obviously, the active power generated by the system ( $P_{R0}^*$ ) should satisfy the inequality:

$$P_{R0}^* \geq P_{WT0}^*.$$

The orthogonal components of voltages in the sections  $S_R$  and  $S_G$  for a given active power are determined, as it follows from (12), according to the expression:

$$u_{Rq0}^* = \omega^* \cdot \left(1 - \frac{P_{R0}^*}{u_{Rd0}^*}\right) \frac{k_L + q}{k_L - 1}; \quad u_{Gq0}^* = \omega^* \cdot \left(1 - \frac{P_{R0}^*}{u_{Gd0}^*(1+q)}\right) \frac{k_L}{k_L - 1};$$

On the other hand, the active power generated by system

$$P_{R0}^* = e_{Gq}^* i_{Gq0}^* = \omega^* i_{Gq0}^* = \omega^* \frac{u_{Rd0}^*}{X_{q\Sigma}^*} = \omega^* \frac{u_{Gd0}^*}{X_q^*} = \frac{1+q}{k_L + q} u_{Rd0}^* = \frac{1+q}{k_L} u_{Gd0}^*. \quad (21)$$

At  $k_L \rightarrow 1$   $P_{R0}^* \approx u_{Rd0}^* = (1+q)u_{Gd0}^*$ .

Fig. 8 shows the dependence  $u_{Rq0}^*$  of  $u_{Rd0}^*$  for different values  $P_{R0}^*$ . Constancy of the active power is carried out on the sites of characteristics between the points of «a» and «b» outside of these points the modulation index (M) is limited and the active power decreases.

The total power and power factor in the section  $S_R$  are defined by the relations:

$$S_{R0}^* = [(Q_{G0}^*)^2 + (P_{G0}^*)^2]^{\frac{1}{2}}, \quad \cos \varphi_R = P_{R0}^* / S_{R0}^*,$$

where the reactive power  $Q_{R0}^*$  is determined by the ratio

$$Q_{R0}^* = \frac{1+q}{\omega^*(k_L + q)} (u_{Rd0}^*)^2 + \frac{1}{\omega^*} (u_{Rq0}^*)^2 - u_{Rq0}^*. \quad (22)$$

On fig. 9, 10 the dependences of  $S_R^*$  and  $\cos(\varphi_R)$  on  $\omega^*$  are presented. As can be seen from figure 9 at a certain frequencies, there is a minimum total power that takes place at zero values of the inactive power. Denote the frequency at which there is a minimum of full power as  $\omega_0^*$ , while its value is determined using the relation

$$\omega_0^* = u_{Rq0}^* + \frac{(u_{Rd0}^*)^2 (1+q)}{u_{Rq0}^* (1+k_L)} = u_{Gq0}^* + \frac{(u_{Gd0}^*)^2}{u_{Gq0}^*} \frac{1}{k_L}$$

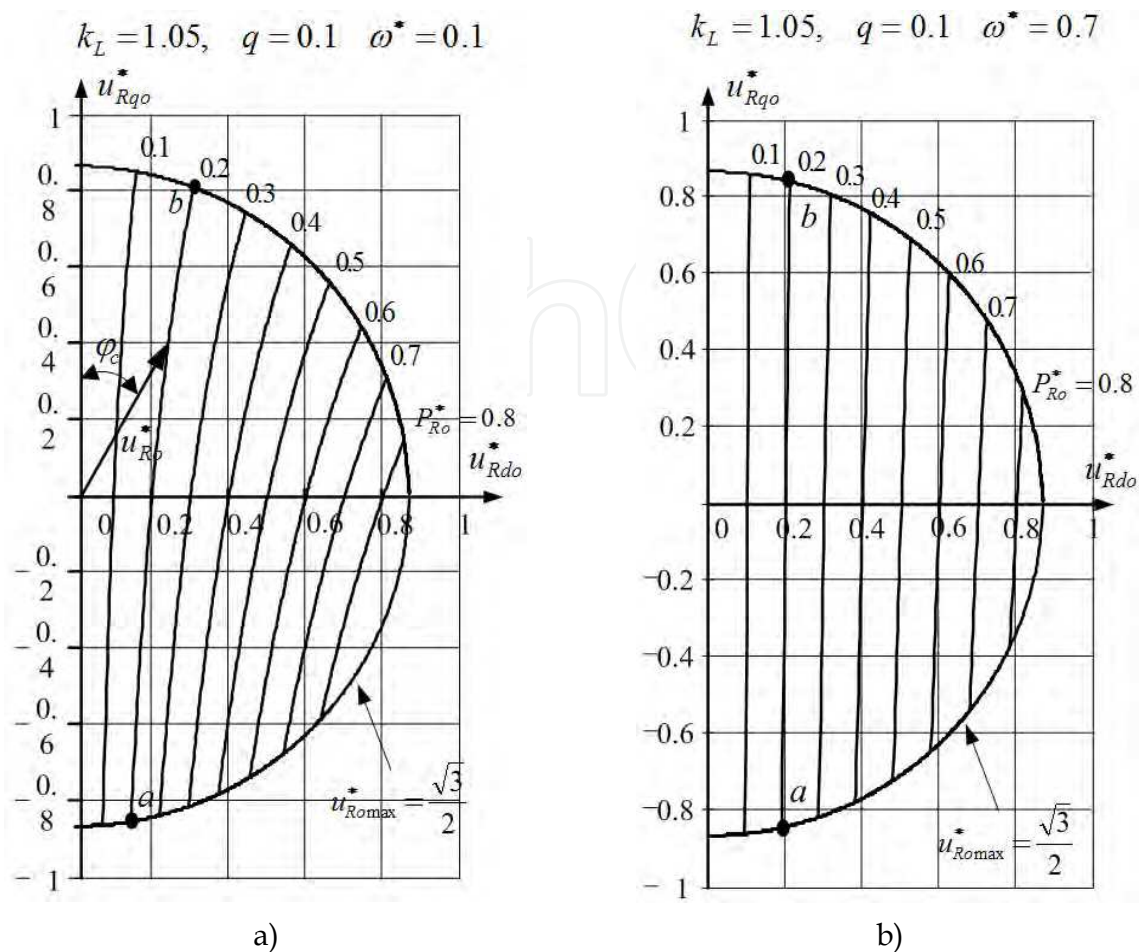


Fig. 8.

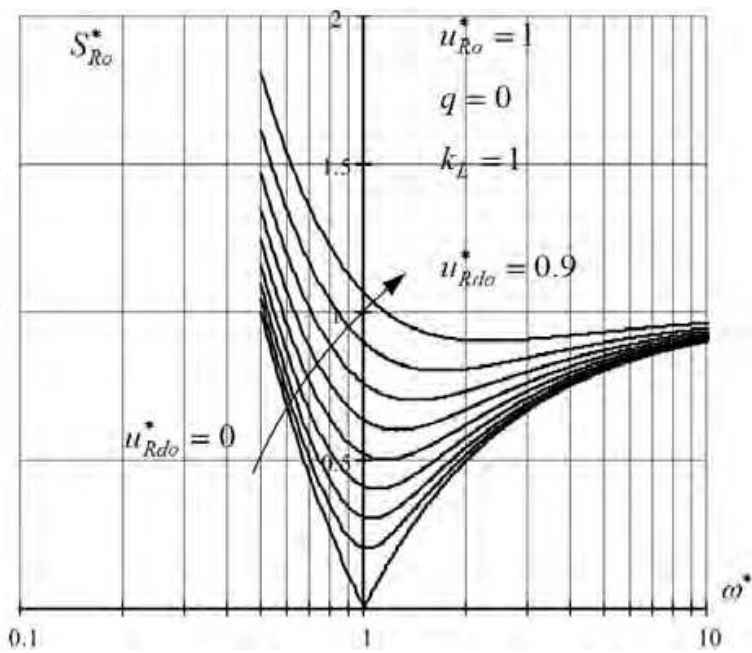


Fig. 9.

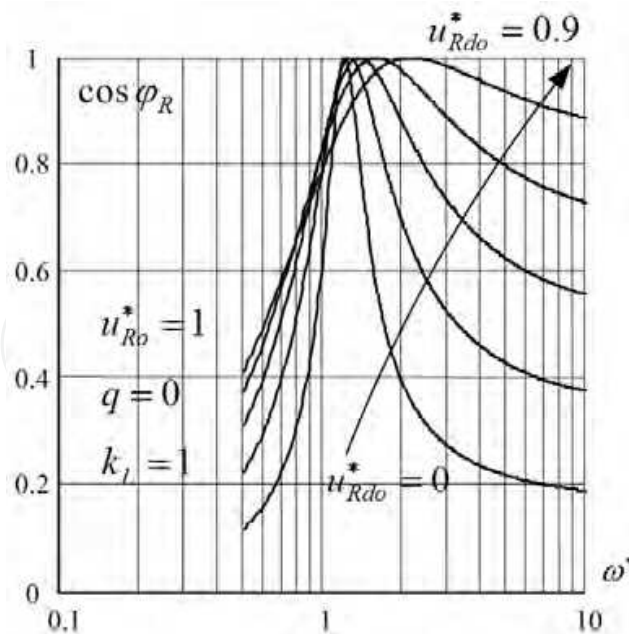


Fig. 10.

As appears from (22), the orthogonal components  $u_{Rdo}^*$  also  $u_{Rqo}^*$  are connected by the equation

$$\left( \frac{u_{Rdo}^*}{\gamma_Q R_Q} \right)^2 + \left( \frac{u_{Rqo}^* - \frac{\omega^*}{2}}{R_Q} \right)^2 = 1, \quad (23)$$

where:

$$\gamma_Q = \sqrt{(k_L + q)/(1 + q)}, \quad R_Q = \sqrt{\omega^* Q_{Ro}^* + (\omega^*/2)^2}. \quad (24)$$

Expression (23) is the equation of an ellipse with the major axis  $-2a_d$  and the minor axis  $-2b_q$  that we find from the following expressions:

$$a_d = \gamma_Q R_Q; \quad b_q = R_Q.$$

Thus the ellipse centre in « $d q$ » co-ordinates is located in a point  $(0, \omega^*/2)$ .

Considering the known relation [8], equation (23) in polar coordinates takes the form:

$$\rho(\phi)^2 \cdot [1 - (\varepsilon \cos \phi)^2] - 2\rho_{ucr}(\phi)\rho_0 \left[ \left( \frac{b_q}{a_d} \right)^2 \cos \phi \cos \phi_0 + \sin \phi \sin \phi_0 \right] + \rho_0^2 \cdot [1 - (\varepsilon \cdot \cos \phi_0)^2] - b_q^2 = 0,$$

where co-ordinates of the centre of the ellipse  $\rho_0, \phi_0$  and the parameter  $\varepsilon$  are defined by means of expressions

$$\rho_0 = \frac{n^*}{2}; \quad \phi_0 = \frac{\pi}{2}; \quad \varepsilon^2 = 1 - \left( \frac{b_q}{a_d} \right)^2 = \frac{k_L - 1}{k_L + q}. \quad (25)$$

Considering (24) ÷ (25) we will obtain the following expression for the locus of voltage

$$u_{R0}^* = \sqrt{(u_{Rdo}^*)^2 + (u_{Rq0}^*)^2} \text{ in section } S_R^*$$

$$u_{R0}^* = \left[ \omega^* \sin \phi + \sqrt{(\omega^* \sin \phi)^2 + 4\omega^* Q_{R0}^* (1 - \varepsilon^2 \cos \phi)} \right] / \left[ 2(1 - \varepsilon^2 \cos \phi) \right]; \quad \phi \in (0, 2\pi).$$

The dependence  $u_{R0}^*(\phi)$  for different values  $\omega^*$  and the value of reactive power  $Q_{R0}^*$  are shown in Figure 11. Here and below, a circle with a radius  $u_{R0\max}^* = \sqrt{3}/2$  is limiting mode with  $M = 1$ , i.e. outside this circle the modulation depth is limited, and therefore the ratios obtained above are valid only inside the circle. The negative value of the reactive power  $Q_{R0}^*$  means that in the given section the current of the basic harmonic lags behind of a voltage phase.

Considering  $P_{R0}^* \approx u_{Rdo}^*$ , from fig. 11b it follows that the maximum active power ( $P_{R0\max}^*$ ) which is defined by the maximum projection of locus on a «d» axis, essentially depends on size of the reactive power ( $Q_{R0}^*$ ), and at a negative value of  $Q_{R0}^*$   $P_{R0\max}^*$  decreases. Indeed from (23) and (24) we obtain:

$$P_{R0\max}^* \approx \gamma_Q R_Q \approx \sqrt{\omega^* Q_{R0}^* + (\omega^*/2)^2}.$$

By changing the coordinates  $u_{Rdo}^*, u_{Rq0}^*$  we obtain the possibility to control the active power generated and the reactive power consumed from the generator on the fundamental harmonic.

Using the relation  $Q_{R0}^* = tg\varphi_{SR} P_{R0}^*$  and assuming  $q = 0$  that equation (23) can be rewritten in the variables  $P_{R0}^*$  and  $u_{Rq0}^*$

$$\left( \frac{P_{R0}^* - \frac{\omega^*}{2} tg\varphi_{SR} \cdot k_L}{\sqrt{k_L} \cdot \frac{\omega^*}{2} \sqrt{1 + k_L (tg\varphi_{SR})^2}} \right)^2 + \left( \frac{u_{Rq0}^* - \frac{\omega^*}{2}}{\frac{\omega^*}{2} \sqrt{1 + k_L (tg\varphi_{SR})^2}} \right)^2 = 1 \tag{26}$$

$$a_d = \frac{\omega^*}{2} \sqrt{k_L} \sqrt{1 + k_L (tg\varphi_{SR})^2}; \quad b_q = \frac{\omega^*}{2} \sqrt{1 + k_L (tg\varphi_{SR})^2}.$$

Thus the ellipse centre in «d q» co-ordinates is located in a point  $(\omega^* tg\varphi_{SR} \cdot k_L \cdot (1 + q)/2, \omega^*/2)$

$$\rho_0 = \frac{n^*}{2} \sqrt{1 + (tg\varphi_{SR} \cdot k_L)^2}; \quad \phi_0 = arctg\left(\frac{1}{tg\varphi_{SR} \cdot k_L}\right); \quad \varepsilon^2 = 1 - \left(\frac{b}{a}\right)^2 = \left(1 - \frac{1}{k_L(1+q)^2}\right).$$

The maximum active power generated for the each set of parameters is determined by the point on the graph, as shown, for example, in fig.12a. From the relation (26) we obtain

$$P_{R0\max}^* = a_d + \omega^* k_L tg\varphi_{SR} / 2 = \omega^* / 2 [\sqrt{k_L} tg\varphi_{SR} + \sqrt{1 + k_L (tg\varphi_{SR})^2}].$$

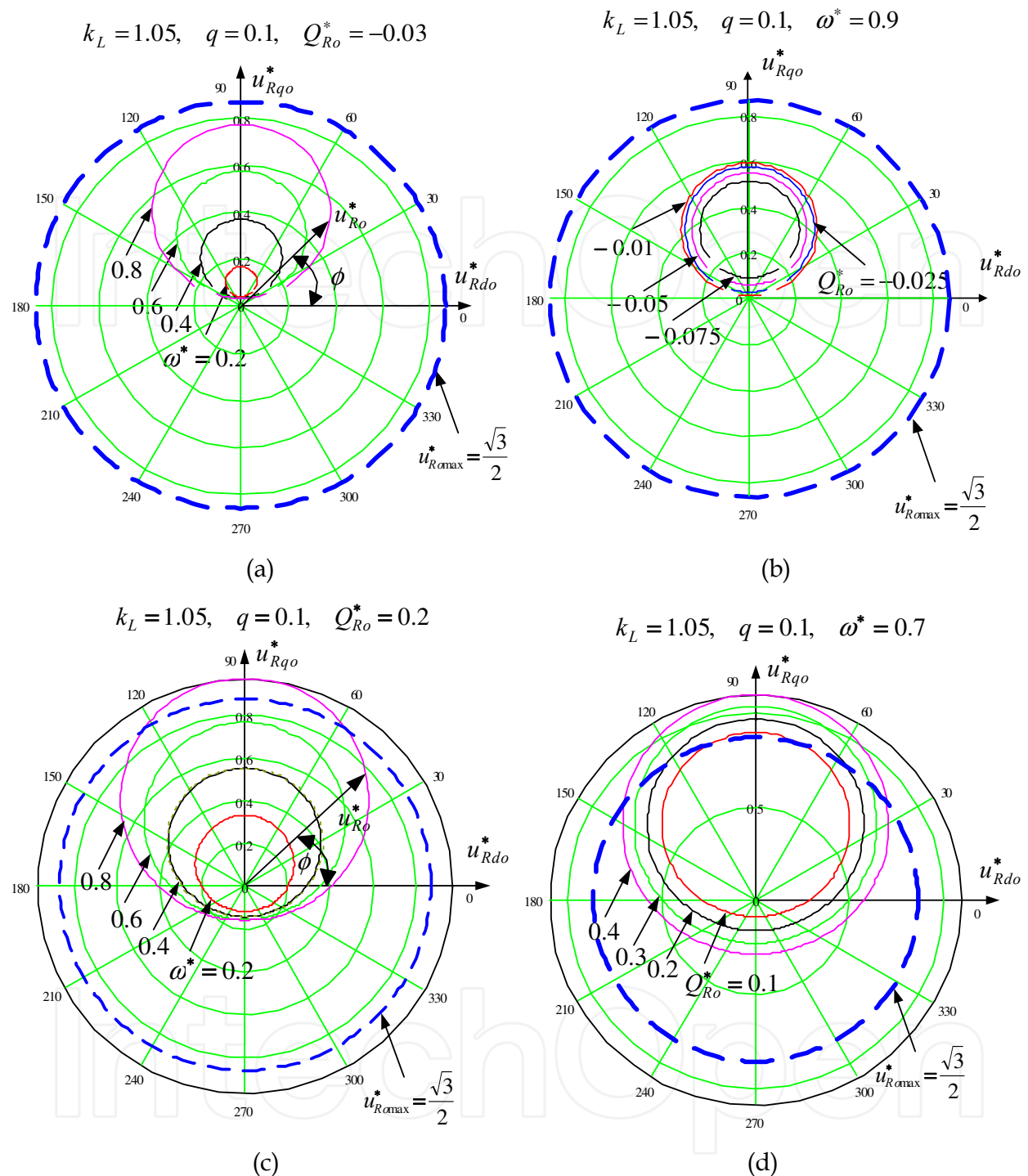


Fig. 11.

The graph of dependence  $P_{Rmax}^*$  on the frequency of rotation  $\omega^*$  and  $\phi_{SR}$  for the various  $k_L$  is presented in fig. 13.

The above reasoning and results of calculations allow drawing a conclusion that thanks to possibility of independent regulation by means of the active rectifier of orthogonal components of the resultant voltage vector  $u_R$ , modes with various  $\cos(\phi_R)$  values at change  $\omega^*$  are possible in the system.

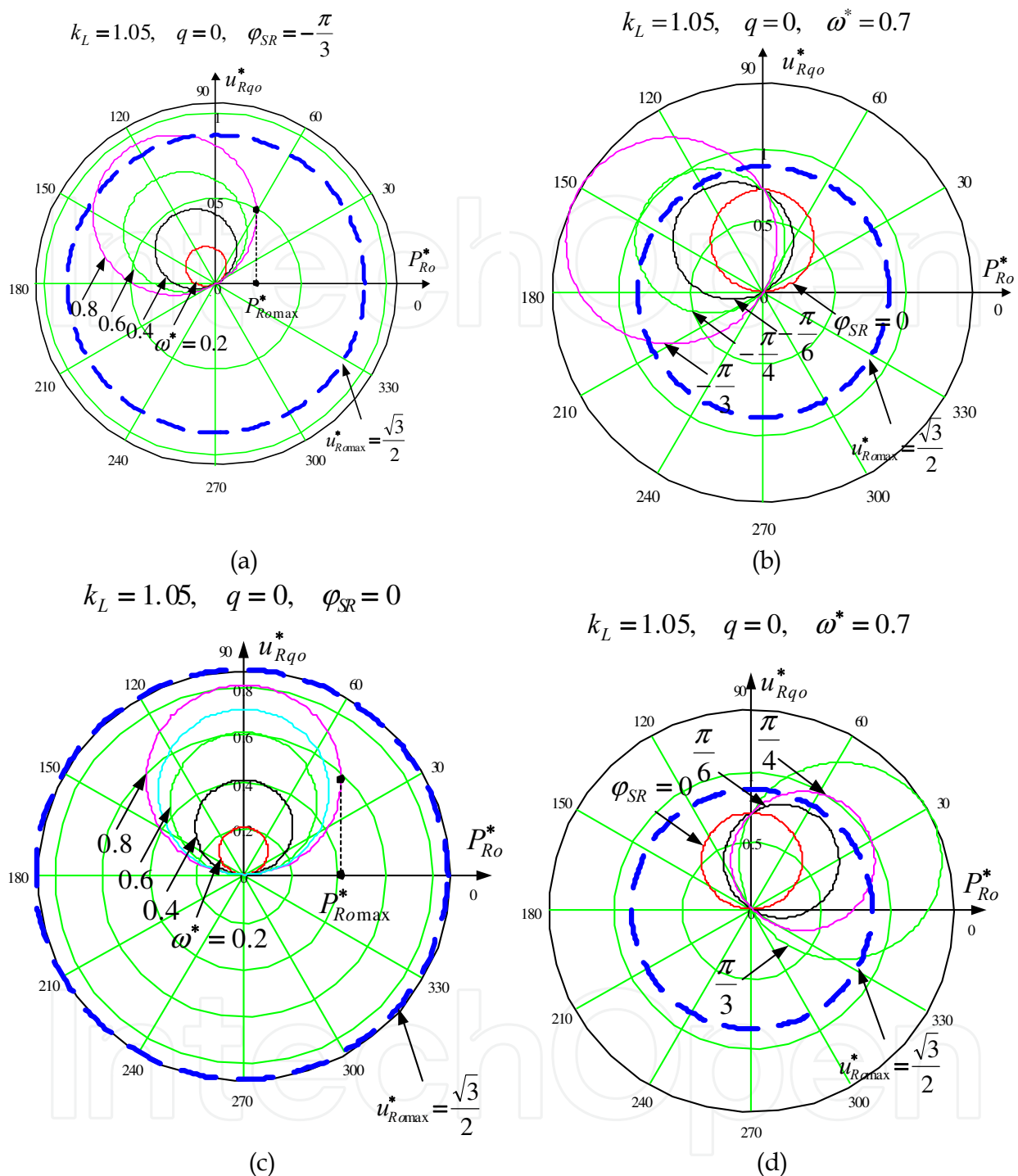


Fig. 12.

**Phases of the fundamental harmonics of current and voltage of the generator coincide.**

The vector diagram for the fundamental harmonics of current and voltage in the given mode is shown in fig. 14. As appears from the given diagram

$$\text{tg}(\theta) = i_{do}^* / i_{qo}^* = u_{gdo}^* / u_{gqo}^* .$$

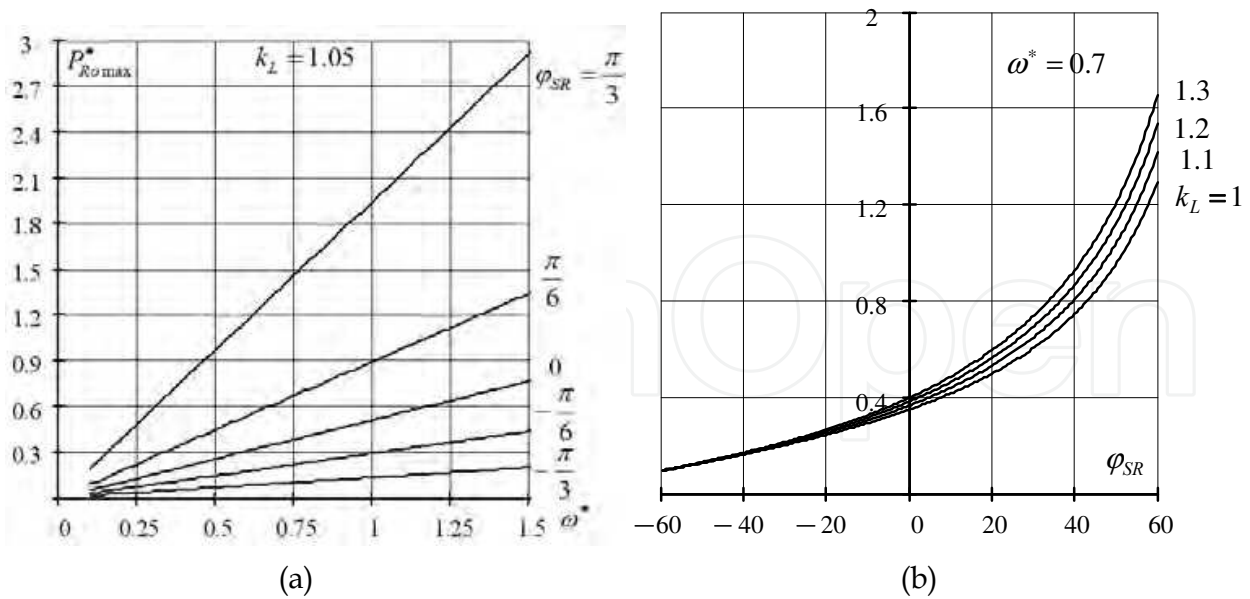


Fig. 13.

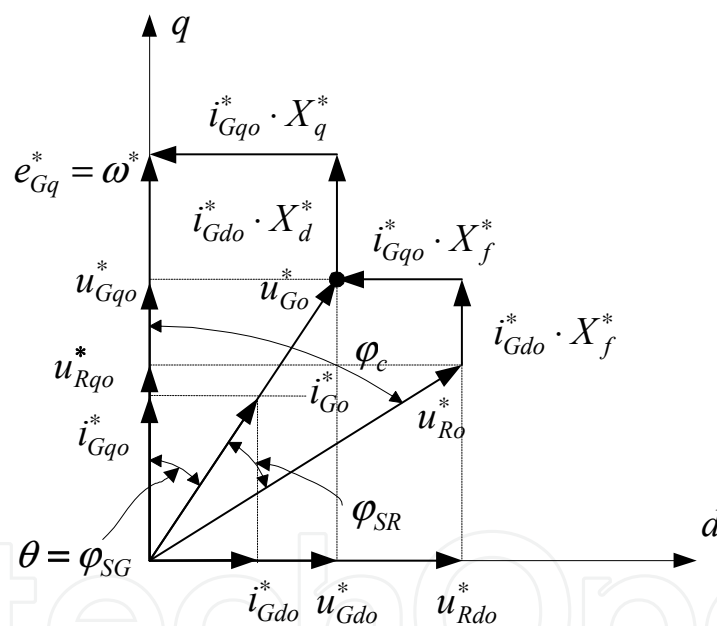


Fig. 14.

This ratio provides a functional link between the orthogonal components  $u_{do}^* = \sqrt{3}M_d/2$  and  $u_{qo}^* = \sqrt{3}M_q/2$ . For this we use the relations (16) and (17), as a result we obtain:

$$\frac{\omega^* - u_{Rqo}^* \cdot \frac{k_L + q}{1 + q}}{u_{Rdo}^*} = \frac{\gamma_q u_{Rdo}^*}{\gamma_d u_{Rqo}^* + (1 - \gamma_d)\omega^*}, \tag{27}$$

where  $\gamma_q = X_q/X_{q\Sigma} = k_L/(k_L + q)$ ,  $\gamma_d = X_d/X_{d\Sigma} = 1/(1 + q)$ .

Expression (27) represents the ellipse equation, in a canonical form this equation will become:

$$\frac{(u_{Rdo}^*)^2}{(\gamma_u R)^2} + \frac{(u_{Rqo}^* + u_{0q}^*)^2}{R^2} = 1, \tag{28}$$

where the semi-major axis  $a_d = \gamma_u R$  and semi-minor axis  $b_q = R$ , values of  $\gamma_u$ ,  $R$  and  $u_{0q}^*$  are determined by the relations:

$$\gamma_u = \frac{k_L + q}{1 + q} \cdot \frac{1}{\sqrt{k_L}}; R = \frac{\omega^*}{2}(1 + q); u_{0q}^* = \frac{\omega^*}{2}(q - 1).$$

The equation (28) in polar co-ordinates looks like:

$$u_{Ro}^* = \sqrt{(u_{do}^*)^2 + (u_{qo}^*)^2} = \frac{\omega^*}{2} \frac{-(q-1)\sin\phi + \sqrt{(q-1)^2 \sin^2\phi + 4q \cdot (1 - \varepsilon^2 \cos^2\phi)}}{1 - \varepsilon_{Ro}^2 \cos^2\phi}, \phi \in (0, 2\pi), \tag{29}$$

where  $\varepsilon_{Ro}^2 = \begin{cases} 1 - \frac{(\gamma_u R)^2}{R^2} = 1 - (\gamma_u)^2 = 1 - \left(\frac{k_L + q}{1 + q}\right)^2 \frac{1}{k_L}, \text{если } q > \sqrt{k_L}; \\ 1 - \frac{R^2}{(\gamma_u R)^2} = 1 - \frac{1}{(\gamma_u)^2} = 1 - \left(\frac{1 + q}{k_L + q}\right)^2 k_L, \text{если } q < \sqrt{k_L}. \end{cases}$

The character of change  $u_{Ro}^*$  as the function of  $\phi$  is shown in fig.15.

In figure 16 the loci are constructed in accordance with the relation (29) for the different values of  $\omega^*$ ,  $q$  and  $k_L$ . With the increase of  $q$  (fig.16a), with the same value  $u_{Rdo}^* \equiv P_{Ro}^*$ , the coordinate  $u_{Rqo}^*$  changes sign and increases the module.

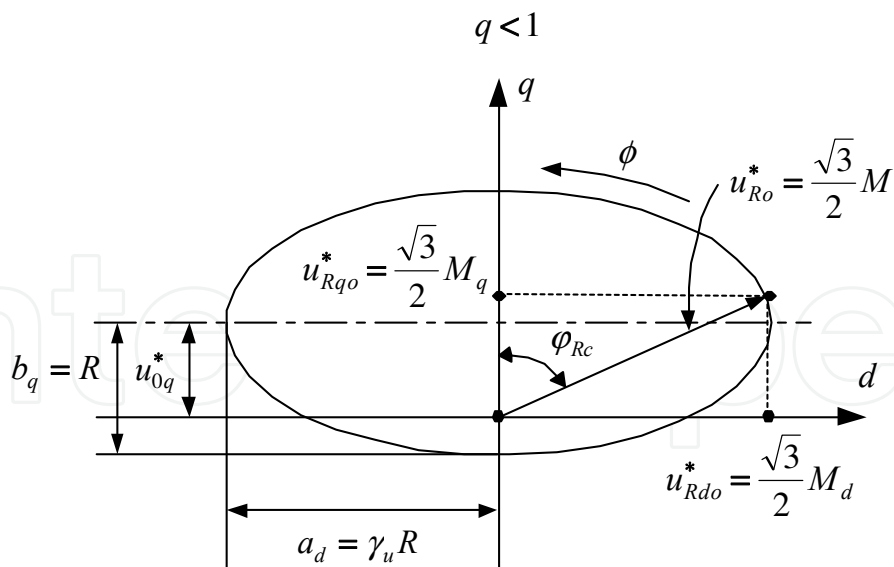


Fig. 15.

At  $k_L \rightarrow 1$  (fig.16) the loci are circles, while it should be noted that when  $k_L = 1 \div 1.1$  you can take  $k_L = 1$ . At a constant  $\omega^*$  in this mode, the voltage module  $u_{Ro}^*$  increase should be accompanied by the growth of the both orthogonal components  $u_{do}^*$  and  $u_{qo}^*$ .

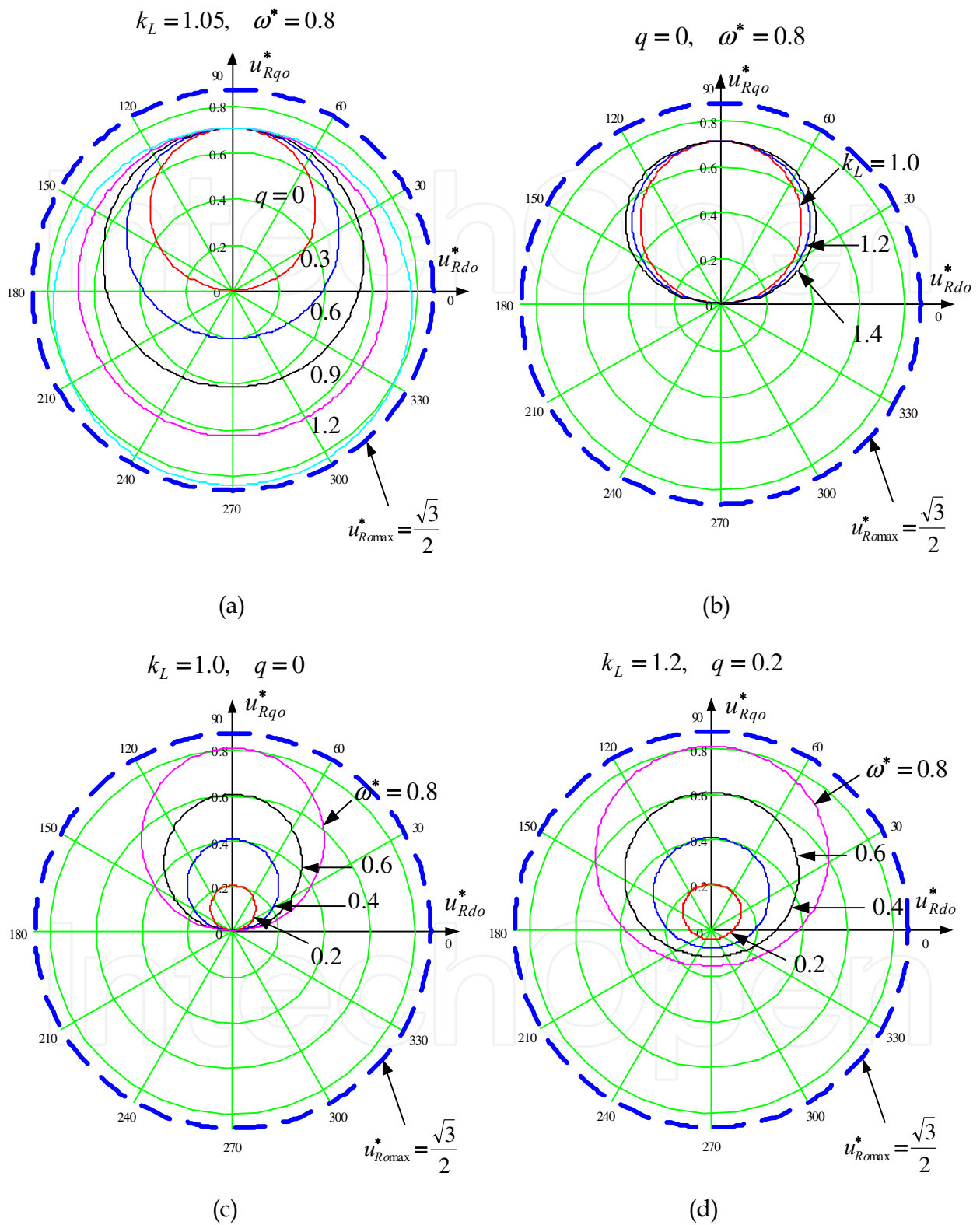


Fig. 16.

The loci of voltage and current of the generator in this mode are determined by the following relations:

$$\left(\frac{u_{Gdo}^*}{\sqrt{k_L} \frac{\omega^*}{2}}\right)^2 + \left(\frac{u_{Gqo}^* - \frac{\omega^*}{2}}{\frac{\omega^*}{2}}\right)^2 = 1, \quad u_{Go}^* = \frac{\omega^* k_L \sin \phi +}{k_L \sin \phi^2 + \cos \phi^2},$$

$$\left(\frac{i_{do}^* - \frac{1+q}{2}}{\frac{1+q}{2}}\right)^2 + \left(\frac{i_{qo}^*}{\frac{1+q}{2} \frac{1}{\sqrt{k_L}}}\right)^2 = 1, \quad i_{Go}^* = \frac{\cos \phi \cdot (q+1)}{k_L \sin \phi^2 + \cos \phi^2}. \quad (30)$$

The three loci ( $u_{Go}^*, u_{Ro}^*, i_{Go}^*$ ), built on the same graph, are shown in figure 17.

From the graph and the relation (30) it follows that the maximum values of a current in orthogonal axes are:

$$i_{do\max}^* = (1+q)/2; \quad i_{qo\max}^* = (1+q)/2\sqrt{k_L}. \quad (31)$$

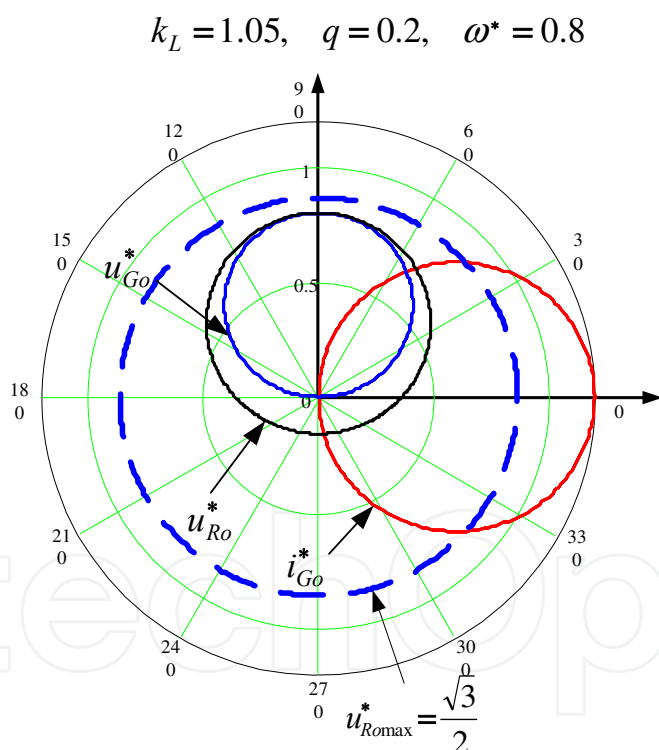


Fig. 17.

Taking into account, that

$$P_{Ro}^* = \frac{P_{Ro} \omega_b L_d (1+q)}{E_b^2} = \frac{1+q}{k_L + q} u_{Rdo}^* = \frac{\sqrt{3}}{2} \frac{1+q}{k_L + q} M_d,$$

Equation (28) can be rewritten in the coordinates ( $P_{Ro}^*, u_{Rqo}^*$ )

$$\frac{(P_{Ro}^*)^2}{\left(\frac{R}{\sqrt{k_L}}\right)^2} + \frac{(u_{Rqo}^* + u_{0q}^*)^2}{R^2} = 1, \quad (32)$$

$$R = \frac{\omega^*}{2}(1+q); u_{0q}^* = \frac{\omega^*}{2}(q-1).$$

$$\sqrt{(P_{Ro}^*)^2 + (u_{Rqo}^*)^2} = \omega^* \cdot \frac{(1-q)\sin\phi + \{[(1+q)\sin\phi]^2 + 4qk_L(\cos\phi)^2\}^{\frac{1}{2}}}{2[(\sin\phi)^2 + (\cos\phi)^2 k_L]}.$$

The graph of  $u_{Rqo}^*$  change at a variation of  $P_{Ro}^*$  is shown in fig. 18.

$$k_L = 1.05, \quad q = 0.2$$

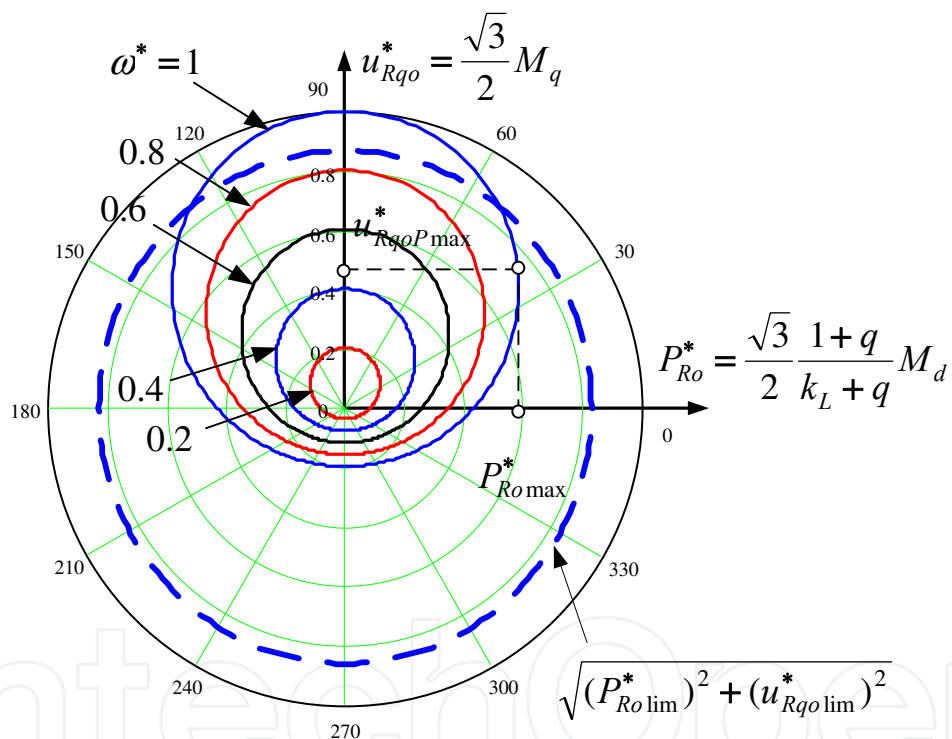


Fig. 18.

The limiting locus is determined by the condition

$$M_d^2 + M_q^2 \leq 1,$$

whence we obtain

$$\frac{(P_{Ro}^* \lim)^2}{\left(\frac{1+q}{k_L+q} \frac{\sqrt{3}}{2}\right)^2} + \frac{(u_{Rqo}^* \lim)^2}{\left(\frac{\sqrt{3}}{2}\right)^2} = 1. \quad (33)$$

$$\sqrt{(P_{Ro\lim}^*)^2 + (u_{Rqo\lim}^*)^2} = \frac{\sqrt{3}}{2} \frac{1}{\sqrt{\left(\frac{k_L + q}{1 + q}\right)^2 (\cos\phi)^2 + (\sin\phi)^2}}.$$

For a given active power  $P_{Ro}^*$  limiting the value of the modulation of control input wave on the transverse axis ( $q$ ) is determined using the relation

$$M_{q\lim} = \sqrt{1 - \left[ \frac{2}{\sqrt{3}} \frac{(k_L + q)}{(1 + q)} P_{Ro}^* \right]^2}.$$

As appears from fig.18, with increasing of the frequency of rotation of the shaft WT ( $\omega^*$ ) there is an increase in active power and for each the value  $\omega^*$  holds the maximum value of active power  $P_{Ro\max}^*$ , which is defined by the relation:

$$P_{Ro\max}^* = \frac{P_{Ro\max} \omega_{\delta}^2 L_d (1 + q)}{E_{\delta}^2} = \frac{\omega^*}{2\sqrt{k_L}} (1 + q) = \frac{\sqrt{3}}{2} \frac{1 + q}{k_L + q} M_{dP\max}, \quad (34)$$

while taking into account the introduced relative units (9), the real value of power can be found from the expression:

$$P_{Ro\max} = E_{\delta}^2 / \omega_{\delta}^2 L_d \cdot \omega^* / 2\sqrt{k_L}.$$

The maximum power is achieved with the following voltage  $u_{Rqo}^* = u_{RqoP\max}^*$  and  $u_{Rdo}^* = u_{RdoP\max}^*$  and also voltage  $u_{Ro}^* = u_{RoP\max}^*$ :

$$u_{RqoP\max}^* = -u_{oq}^* = \frac{\omega^*}{2} (1 - q) = \frac{\sqrt{3}}{2} M_{qP\max}, \quad u_{RdoP\max}^* = \frac{\omega^*}{2} \frac{k_L + q}{\sqrt{k_L}} = \frac{\sqrt{3}}{2} M_{dP\max}, \quad (35)$$

$$u_{RoP\max}^* = \sqrt{(u_{RqoP\max}^*)^2 + (u_{RdoP\max}^*)^2} = \frac{\omega^*}{2} \cdot \sqrt{(q - 1)^2 + \frac{(k_L + q)^2}{k_L}}.$$

At this point the generator voltage in accordance with (35) and (18) is determined by the relations:

$$u_{GqoP\max}^* = \omega^* / 2, \quad u_{GdoP\max}^* = \omega^* k_L (1 - q) / 2(k_L + q),$$

$$u_{GoP\max}^* = \sqrt{(u_{GqoP\max}^*)^2 + (u_{GdoP\max}^*)^2} = \frac{\omega^*}{2} \cdot \sqrt{1 + \left[ \frac{k_L (1 - q)}{k_L + q} \right]^2}. \quad (36)$$

In accordance with (34) and (35) the parameters of control signals for the point with maximum capacity are determined by the following relations

$$M_{dP\max} = \frac{\omega^*}{\sqrt{3}} \cdot \frac{k_L + q}{\sqrt{k_L}}; \quad M_{qP\max} = \frac{\omega^*}{\sqrt{3}} \cdot (1 - q);$$

$$M_{P_{\max}} = \frac{\omega^*}{\sqrt{3}} \cdot \sqrt{(q-1)^2 + \frac{(k_L+q)^2}{k_L}}; \quad \varphi_{RcP_{\max}} = \arctg \left[ \frac{M_{dP_{\max}}}{M_{qP_{\max}}} \right] = \arctg \left[ \frac{k_L+q}{\sqrt{k_L} \cdot (1-q)} \right];$$

Dependence of the active power on the frequency of rotation ( $\omega^*$ ), values of the modulation depth of control input wave on the transverse axis ( $M_q$ ) and parameters  $k_L$  and  $q$  is defined as follows:

$$P_{Ro}^* = \frac{1}{\sqrt{k_L}} \left\{ \left( \frac{\omega^*}{2} \right)^2 - \left[ \frac{\sqrt{3}}{2} M_q + (q-1) \frac{\omega^*}{2} \right]^2 \right\}^{\frac{1}{2}}.$$

Graphs of the dependence of active power from the values  $\omega^*$ ,  $M_q$  are presented in fig.19.

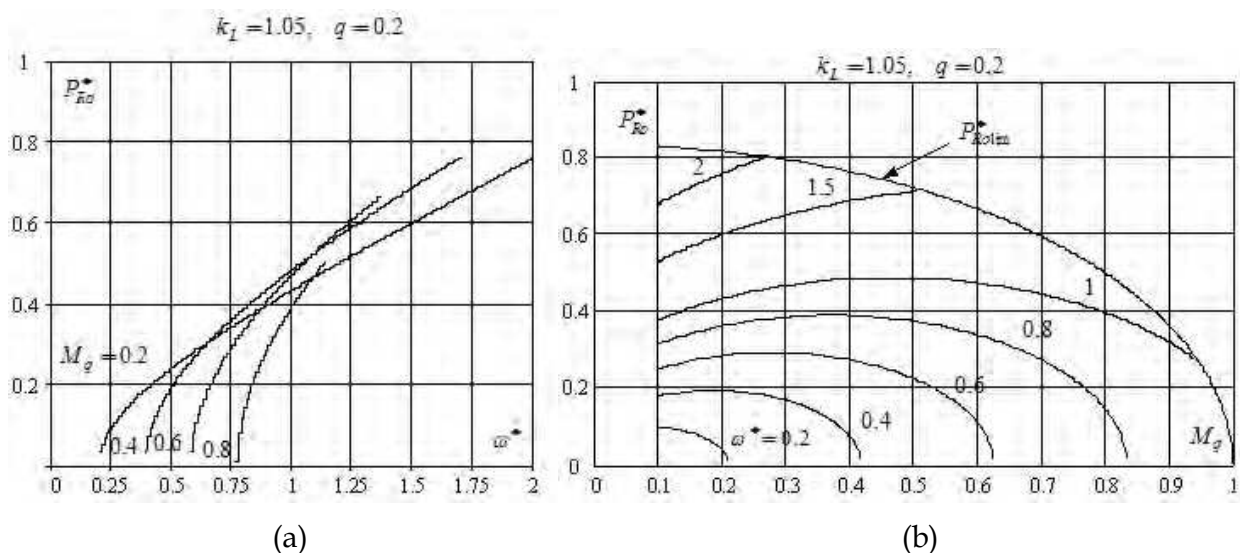


Fig. 19.

As follows from (32a) and fig.19 the same value of active power  $P_{Ro}^*$  can be realized for the two values of voltage along the transverse axis  $u_{Rq0}^*$  (fig.19) - «operating mode 1 and 2». These voltages are defined by the relation

$$u_{Rq01,2}^* = -\frac{\omega^*}{2}(q-1) \mp \sqrt{\left[ \frac{\omega^*}{2}(q+1) \right]^2 - (\sqrt{k_L} P_{Ro}^*)^2}.$$

Considering (18) the generator voltage in these modes will be defined as follows:

$$\begin{aligned} u_{Gq01,2}^* &= \frac{\omega^*}{2} \mp \sqrt{\left( \frac{\omega^*}{2} \right)^2 - \left( \frac{\sqrt{k_L} P_{Ro}^*}{1+q} \right)^2}, \quad u_{Gd0}^* = \frac{k_L}{1+q} P_{Ro}^*, \\ u_{Go1,2}^* &= \frac{\omega^*}{\sqrt{2}} \sqrt{1 + \left( \frac{\sqrt{2k_L} P_{Ro}^*}{(1+q) \cdot \omega^*} \right)^2} (k_L - 1) \mp \sqrt{(1+q)^2 - \left( \frac{2 \sqrt{k_L} P_{Ro}^*}{\omega^* (1+q)} \right)^2}. \end{aligned} \quad (37)$$

$$k_L = 1.0, \quad q = 0, \quad \omega^* = 0.8$$

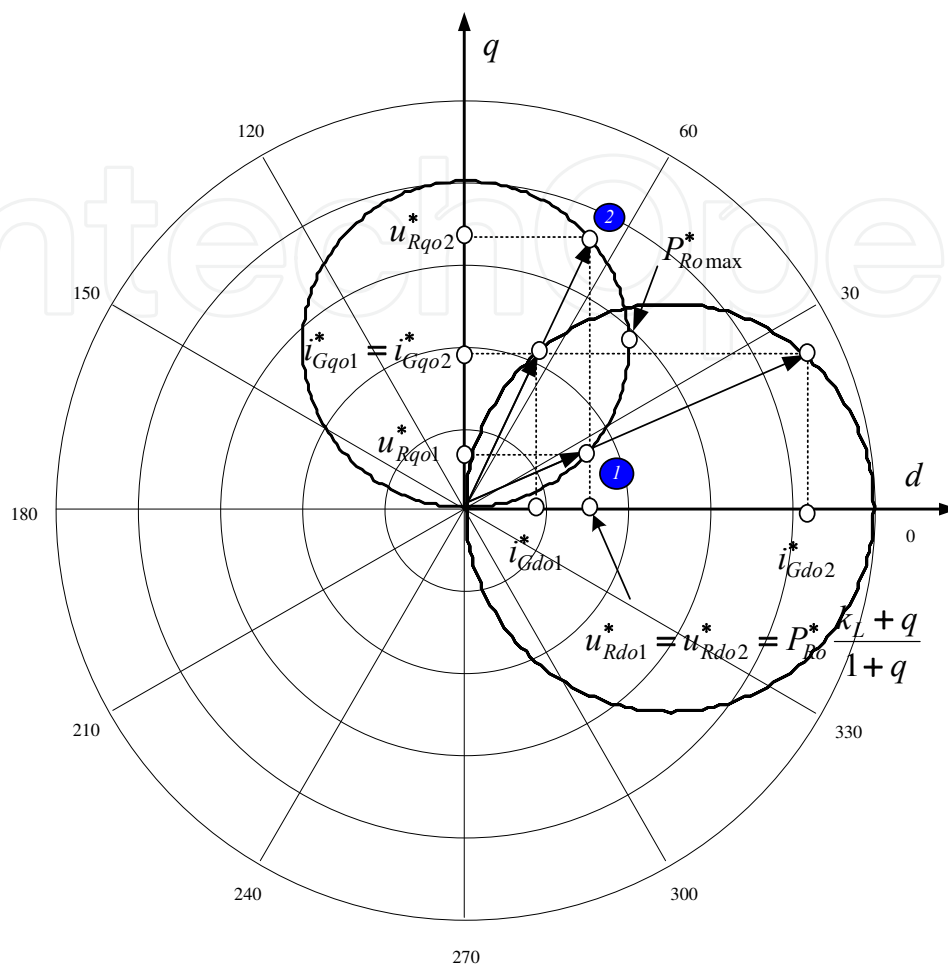


Fig. 20.

From fig.20 it is clear that the larger value of voltage  $u^*$  corresponds to the lower value of current  $i_{G0}^*$ , while  $i_{Gqo1}^* = i_{Gqo2}^*$  that follows from (5a).

$$\begin{cases} i_{Gqo1}^* = i_{Gqo2}^* = u_{Rdo}^* / X_{q\Sigma}^* = P_{Ro}^* / \omega^*, \\ i_{Gdo1,2}^* = 1 - \frac{u_{Rqo1,2}^*}{\omega^*} = \frac{1+q}{2} \pm \sqrt{\left(\frac{1+q}{2}\right)^2 - \left(\frac{\sqrt{k_L} P_{Ro}^*}{\omega^*}\right)^2}. \end{cases}$$

At the point when the power is maximum for a given frequency of rotation ( $P_{Ro}^* = P_{Ro\max}^*$ ), (the relation (34)), the orthogonal components of currents and voltages are determined by the relations (31), (37).

The full value of the generator current is:

$$i_{G01,2}^* = \frac{1+q}{\sqrt{2}} \sqrt{1 + (1-k_L) \left(\frac{2P_{Ro}^*}{\omega^*(1+q)}\right)^2 \pm \sqrt{1 - \left(\frac{2\sqrt{k_L} P_{Ro}^*}{\omega^*(1+q)}\right)^2}}.$$

Graphs of the dependences  $u_{Rq0}^*$ ,  $i_{G0}^*$  and  $u_{G0}^*$  from  $\omega^*$  are presented in fig.30. In these graphs to the right of points «a, b, c, d» there is a limitation of the depth of modulation, and the proposed model becomes inadequate to the real modes.

The first mode on the graphs of fig.21 is characterized by the fact that the generator voltage does not change significantly with variation of  $\omega^*$ . From fig.21d it follows that in mode 1 the system has a positive internal differential resistance and therefore may be potentially unstable at some disturbing effects.

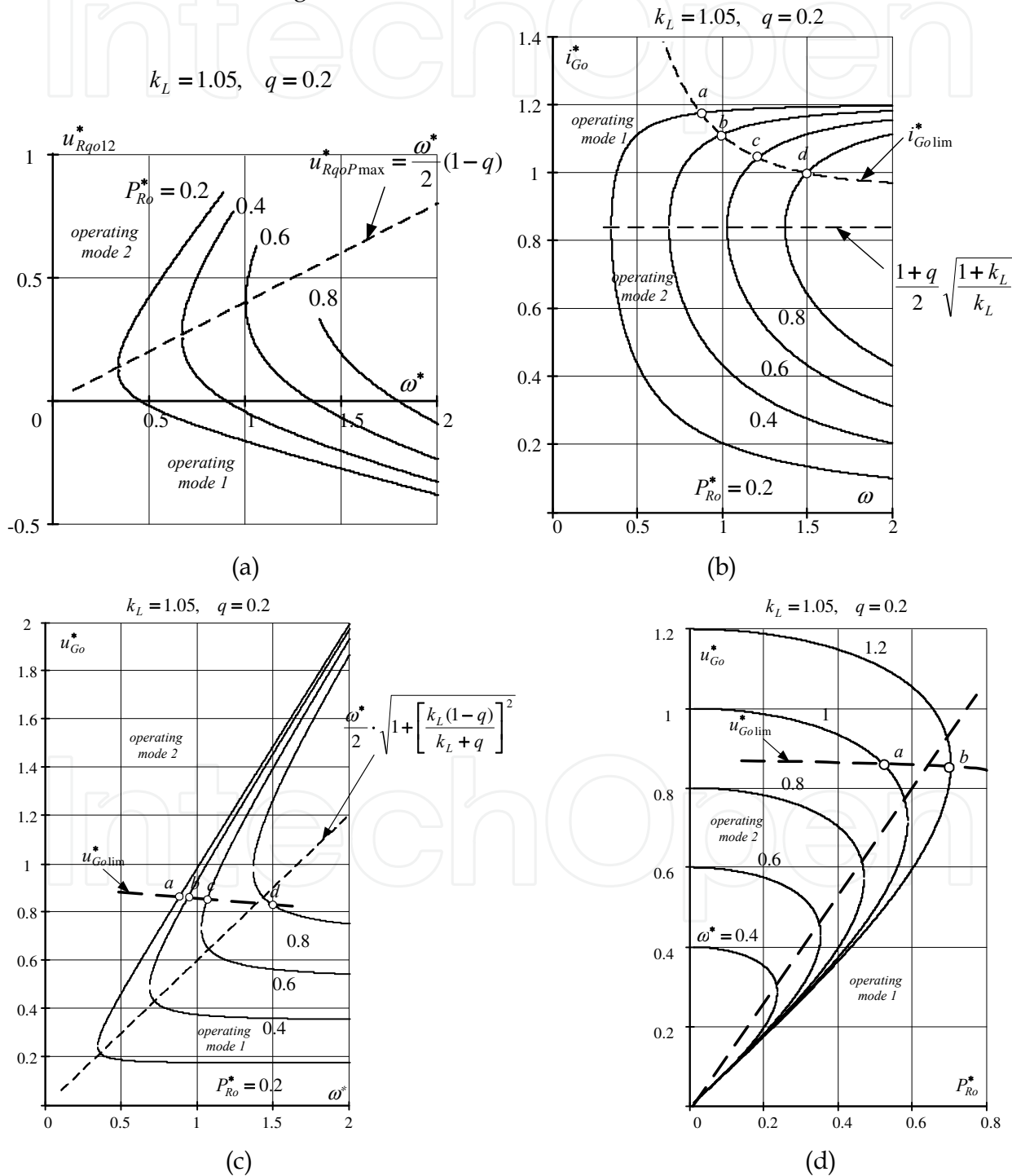


Fig. 21.

It should be noted that the mode when the phases of voltage and current of the fundamental harmonics are the same, essentially involves a change of  $u_{Go}^*$  and  $i_{Go}^*$  under the change of frequency of rotation of the shaft of WT ( $\omega^*$ ).

The equation (28) can be rewritten in the co-ordinates of orthogonal components of a control input wave ( $M_d, M_q$ ):

$$\frac{(M_d)^2}{\left[\gamma_u \frac{\omega^*}{\sqrt{3}}(1+q)\right]^2} + \frac{\left[M_q + \frac{\omega^*}{\sqrt{3}}(q-1)\right]^2}{\left[\frac{\omega^*}{\sqrt{3}}(1+q)\right]^2} = 1, \quad (38)$$

Expression (38) defines a parametric relationship between the orthogonal components, which ensures the phase coincidence of the main of harmonics of the generator voltage and current. This ratio allows us to propose the following control algorithm, in which the active power is given. This solution is useful for the application of the system in the WPI.

In accordance with (16b), (21) and (38), we obtain:

- given the active power -  $P_{Ro}^*$ , when the condition  $P_{Ro\max}^* \leq P_{Ro\max}^* = \omega^*(1+q)/2\sqrt{k_L}$  must be respected;
- the longitudinal component of the modulation ( $M_d$ ) of the control signal is determined by  $M_d = 2(k_L + q)P_{Ro}^*/\sqrt{3}(1+q)$ ;
- the transverse component of the modulation ( $M_q$ ) of the control input wave is

determined by  $M_{q1,2} = -\frac{\omega^*}{\sqrt{3}}(q-1) \mp \sqrt{\left[\frac{\omega^*}{\sqrt{3}}(q+1)\right]^2 - \left(\frac{2}{\sqrt{3}}\sqrt{k_L}P_{Ro}^*\right)^2}$  - here  $M_{q1}$  - corresponds to the mode 1, and  $M_{q2}$  - to the mode 2.

When  $q > 0$ , the fundamental harmonics of inverter current and voltage (section  $S_R$ ) do not coincide in phase. The current phase is ahead of the voltage phase ( $\varphi_{SR} > 0$ ). Fig. 22a shows the dependence of  $\cos \varphi_{SR}$  on the parameters  $q$  and  $k_L$ . From figure 22a it follows that in the first mode there is a significant reduction of  $\cos \varphi_{SR}$  with the increase of the parameter  $q$ . Dependence of  $\cos \varphi_{SR}$  on the parameter  $k_L$  is ambiguous, namely, in the first mode  $\cos \varphi_{SR}$  decreases with the increase of  $k_L$ , while in the second mode, on the contrary increases.

The phases of the fundamental harmonics of generator voltage and current (section  $S_G$ ) are always the same ( $\cos \varphi_{SG} = 1$ ), the power factor in section  $S_G$  will be determined according to (15a) by the relation  $\chi_G = P_{SG}^*/S_{SG}^* = P_{Ro}^*/S_{SG}^* = v_{iG}v_{uG}$ .

The RMS of the fundamental harmonic of generator voltage is determined by the following expression:

$$u_{Go,rms}^* = \frac{1}{\sqrt{2}} \frac{\omega^*}{(q^2 - 1)} \sqrt{q^2 - \left(\frac{\sqrt{3}M}{2\omega^*}\right)^2} \sqrt{\left(\frac{k_L(q+1)}{(k_L+q)}\right)^2 \left[\left(\frac{\sqrt{3}M_{1,2}}{2\omega^*}\right)^2 - 1\right] + \left[q^2 - \left(\frac{\sqrt{3}M_{1,2}}{2\omega^*}\right)^2\right]}. \quad (39)$$

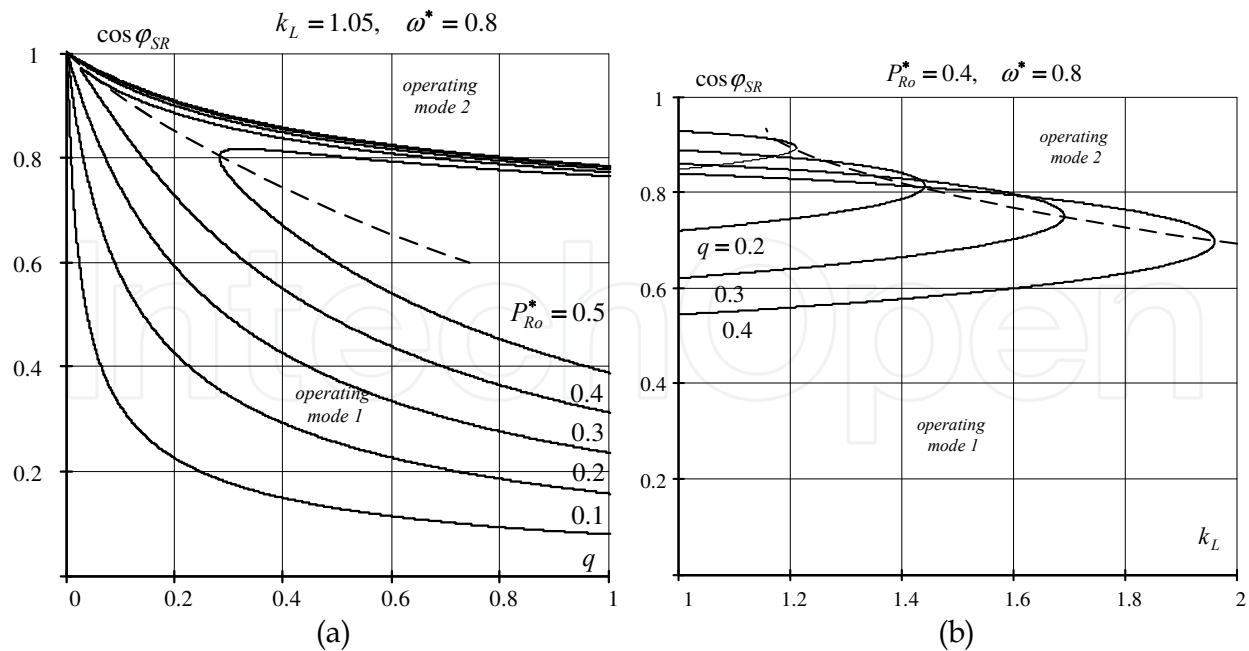


Fig. 22.

Complete RMS of the generator voltage is found from the ratio

$$u_{Go, rms}^* = \frac{1}{\sqrt{2}} \sqrt{(\omega^* \cos \theta)^2 + \frac{M_{1,2}}{(1+q)^2} \left(1 - \frac{3}{4} M_{1,2}\right)}. \quad (40)$$

where:  $\theta$  - the angle shift between the fundamental harmonic of generator voltage and EMF

of generator is defined as follows  $\theta = \arctg \left[ \frac{k_L(1+q)}{k_L+q} \cdot \frac{M_d}{M_{q1,2} + \omega^* \frac{2}{\sqrt{3}}} \right]$ .

The RMS of fundamental harmonic of the generator current

$$i_{Go, rms1,2}^* = \frac{1}{\sqrt{2}} \sqrt{1 - \frac{\sqrt{3}}{\omega^*} M_{q1,2} + \frac{1}{(\omega^*)^2} \left[ \left( \frac{\sqrt{3}}{2} M_{q1,2} \right)^2 + (P_{Ro}^*)^2 \right]} \quad (41)$$

Complete RMS of the generator current is found from the relation (19) and (41).

In fig.23 the distortion coefficients ( $v_{uSG}$ ) and harmonics ( $THD_{uSG}$ ) of generator voltage as functions of the active power generated ( $P_{Ro}^*$ ) and frequency of rotation ( $\omega^*$ ) are presented. As can be seen from fig.23 the best quality of generator voltage is characteristic for mode 2. In addition, analysis of the relations (39) and (40) suggests a reduction factor of harmonics  $THD_{uSG}$  with the increase of the parameter  $q$ . Similar conclusions can be drawn from the consideration of fig. 24, which shows the distortion coefficients ( $v_{iSG}$ ) and harmonics ( $THD_{iSG}$ ) of current as a function of the active power generated ( $P_{Ro}^*$ ) and frequency of rotation ( $\omega^*$ ). In the engineering calculations we can take  $v_{iSG} \approx 1$ .

Power factor of the generator according to (15a), taking into account that  $\cos \phi_{SG} = 1$ , is determined using the relation:  $\chi_G = v_{iG} v_{uG}$ .

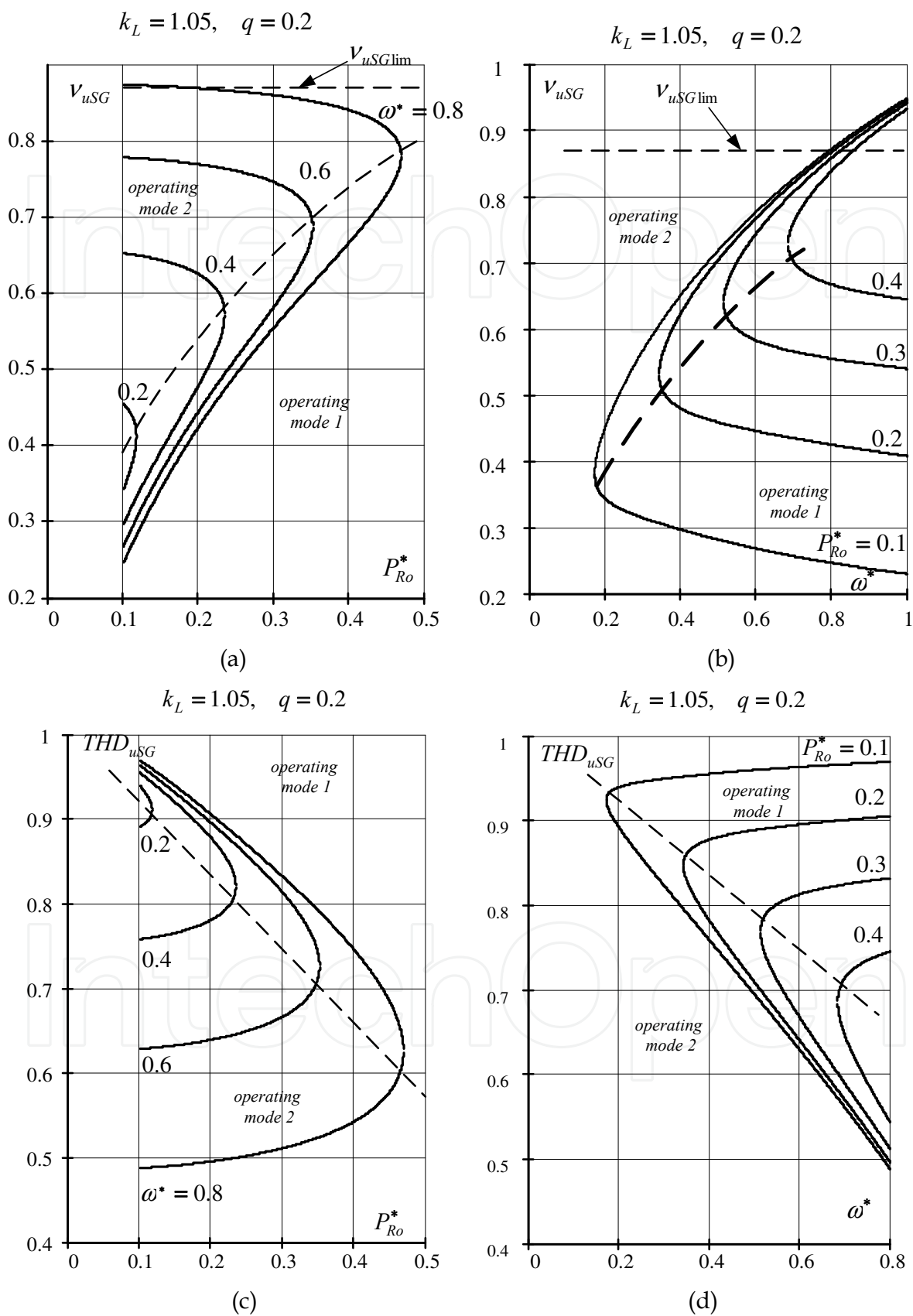


Fig. 23.

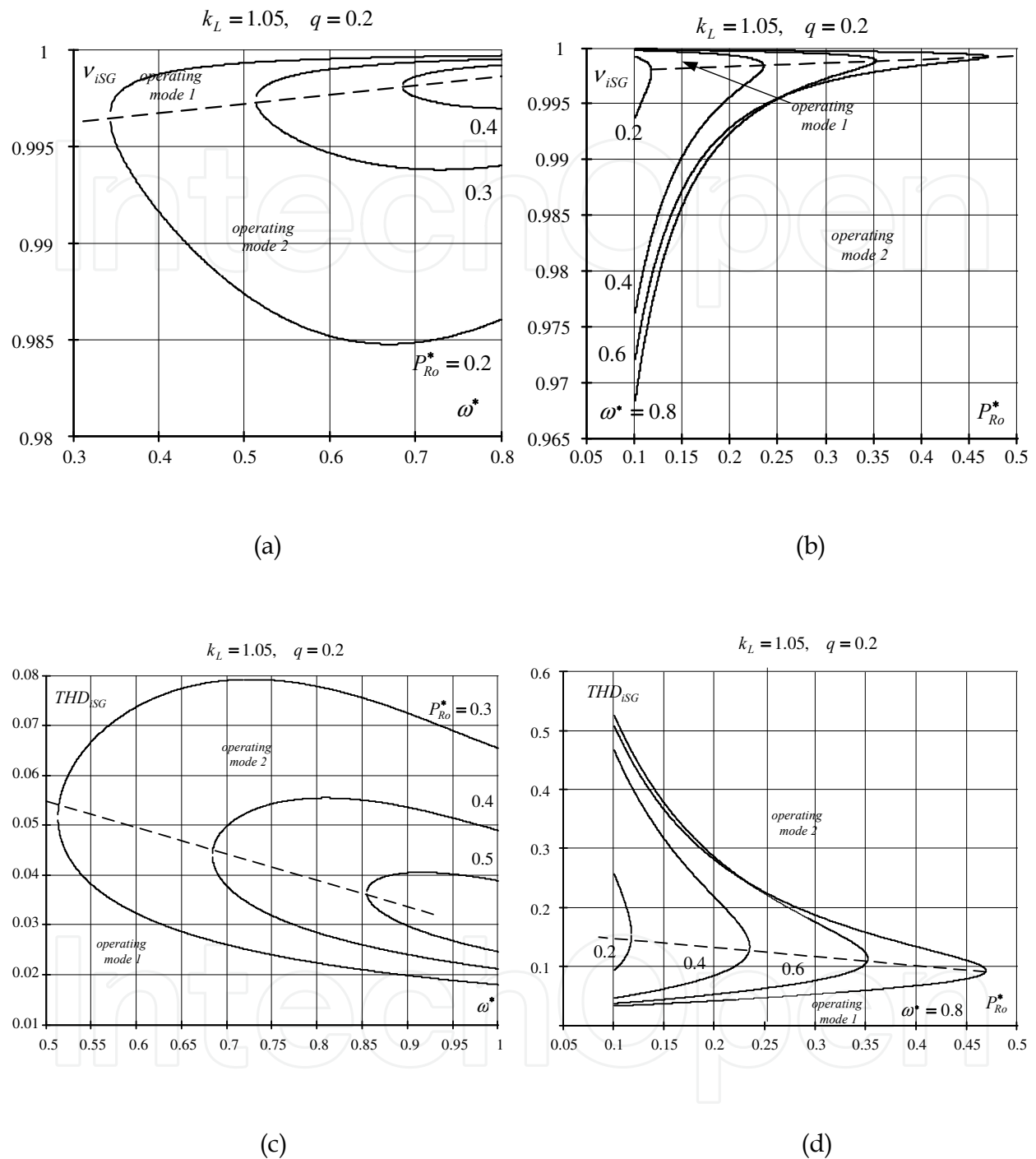


Fig. 24.

Dependence of  $\chi_G$  on the generated active power ( $P_{Ro}^*$ ) and the frequency of rotation ( $\omega^*$ ) is shown in fig.25. From this figure and the previous findings it can be taken:  $\chi_G \approx v_{uG}$ . As expected, the power factor is higher in mode 2. In the mode 1 with a decrease in power  $\chi_G$  is significantly reduced because of the need to reduce the modulation depth  $M$  in order to maintain  $\cos \varphi_{SG} = 1$ .

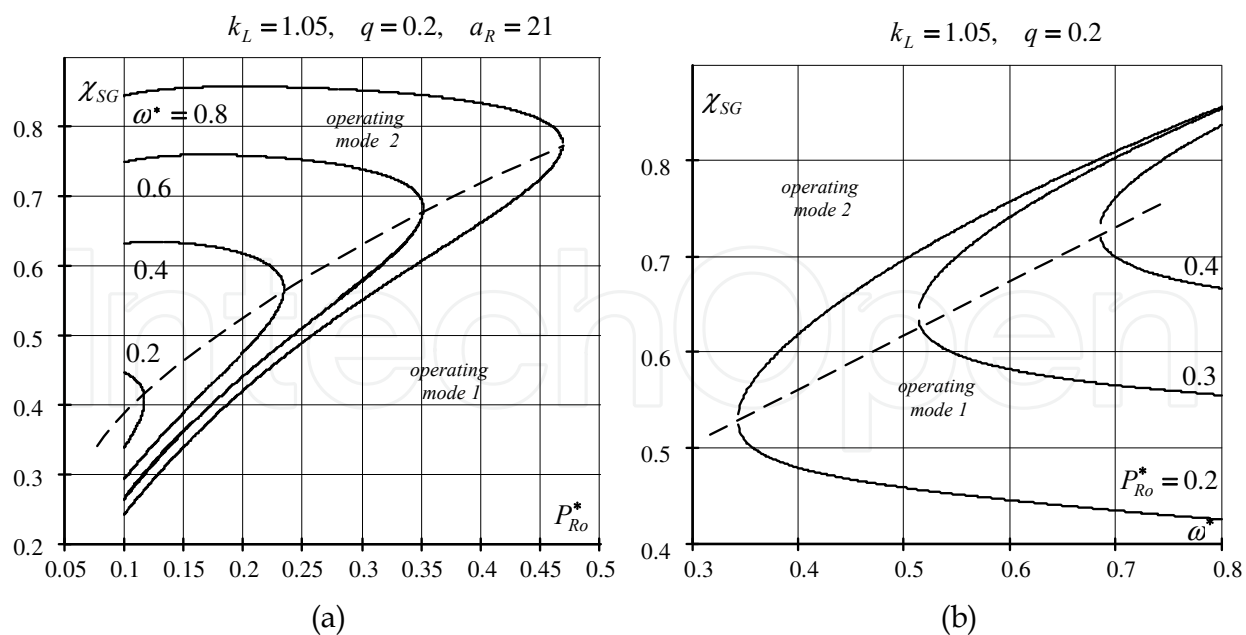


Fig. 25.

From (33), (34) and (35) the conditions can be found under which the maximum power  $P_{Ro\max}^*$  (the point where modes 1 and 2 are the same, fig. 20) is attained at the beginning of the limitations of the modulation depth ( $M=1$ ), i. e.  $P_{Ro\max}^* = P_{Ro\lim}^*$  holds; the value of active power, in the performance of this condition is denoted as  $P_{Ro\max\lim}^*$ .

$$P_{Ro\max\lim}^* = P_{Ro\max}^* = P_{Ro\lim}^* = \frac{\sqrt{3}}{2} \cdot \left\{ \left[ \frac{1-q}{\sqrt{k_L}(1+q)} \right]^2 + \left( \frac{k_L+q}{1+q} \right)^2 \right\}^{-\frac{1}{2}}. \quad (42)$$

The power  $P_{Ro\max\lim}^*$  can be reached at a frequency of rotation  $\omega^* = \omega_{\max\lim}^*$ :

$$\omega_{\max\lim}^* = \sqrt{3} \cdot \left\{ (1-q)^2 + \left( \frac{k_L+q}{\sqrt{k_L}} \right)^2 \right\}^{-\frac{1}{2}}. \quad (43)$$

Taking into account the taken relative units we determine the real value of active power  $P_{Ro\max\lim}$  from the ratio

$$P_{Ro\max\lim} = \frac{E_0^2}{\omega_0 L_d} \cdot \frac{\sqrt{3}}{2} \cdot \left\{ \left( \frac{1-q}{\sqrt{k_L}} \right)^2 + (k_L+q)^2 \right\}^{-\frac{1}{2}}.$$

Figure 26 shows the active power  $P_{Ro\max\lim}/E_0^2/\omega_0 L_d$  and frequency  $\omega_{\max\lim}^*$  as a function of the parameter  $q$  at different values of  $k_L$ .

As can be seen from fig.26, the maximum possible active power ( $P_{Ro\max\lim}^*$ ) and the corresponding speed of rotation in this mode ( $\omega_{\max\lim}^*$ ) occur at  $q = 0, k_L = 1$ . From (42) and (43) we obtain:

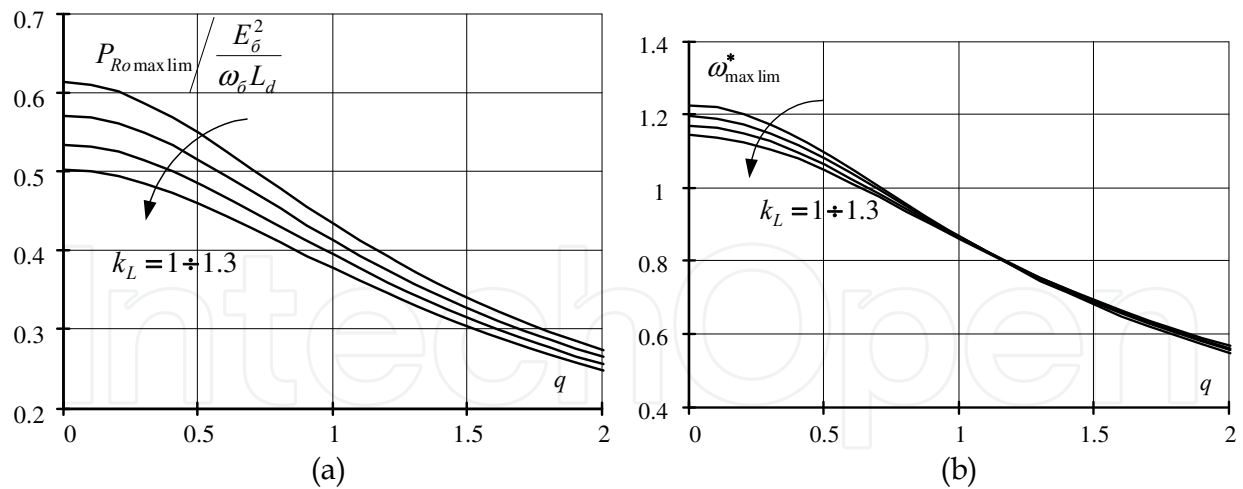


Fig. 26.

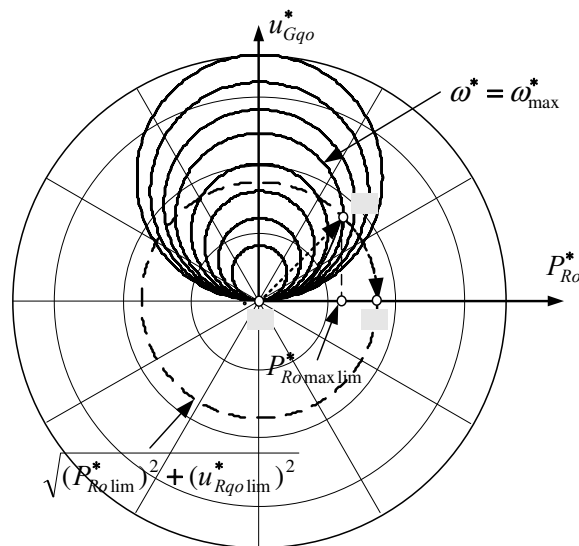


Fig. 27.

$$P_{R_{o\max\lim}}^* = \begin{cases} \sqrt{3}/(2\sqrt{2}) = 0.6124 - \text{SPWM}; \\ 1/\sqrt{2} = 0.7071 - \text{SVPWM}; \end{cases} \quad \omega_{\max\lim}^* = \begin{cases} \sqrt{3}/2 = 1.2247 - \text{SPWM}; \\ \sqrt{2} = 1.4142 - \text{SVPWM}. \end{cases} \quad (44)$$

When we select the power generation system PGS in the WPI, it is convenient to use fig.27. In this figure (for  $q = 0, k_L = 1$ ) the trajectory «  $a \rightarrow b$  » corresponds to the points of maximum power ( $P_{R_{o\max}}^*$ ) for the different frequencies of rotation  $\omega^*$ . At the point «  $b$  »  $P_{R_{o\max}}^* = P_{R_{o\max\lim}}^*$  and  $\omega^* = \omega_{\max\lim}^*$ . With the further increase in frequency  $\omega^*$  to keep the value  $\cos \varphi_{SG} = 1$  without the restrictions of the modulation depth it should be the moving on a trajectory «  $b \rightarrow c$  ». If  $\omega^* \rightarrow \infty$  the point «  $c$  » is reached. The value of active power at the point «  $c$  » will be the maximum possible for  $\cos \varphi_{SG} = 1$ . The value of this power is

$$P_{R_{o\max\lim}}^* (\omega^* \rightarrow \infty) = \begin{cases} \sqrt{3}/2 = 0.866 - \text{SPWM}; \\ 1 - \text{SVPWM}. \end{cases}$$

At work of the PGS from WT an active power will change under the law (20). The mode of the maximum power with  $\omega^* = \omega_{WT\max}^*$  is desirable by choosing from a condition  $\omega_{WT\max}^* = \omega_{\max\lim}^*$ .

In this case according to (20) and (44):

$$P_{WT0\max}^*(\omega_{WT\max}^*) = \gamma \cdot (\omega_{WT\max}^*)^3 = P_{Ro\max\lim}^* ;$$

$$\gamma = P_{Ro\max\lim}^* / (\omega_{WT\max}^*)^3 .$$

When we change  $\omega^*$  the operating point should move along the trajectory «  $a \rightarrow b$  » fig.28, where the power varies according to the law (20), but  $\cos \varphi_{SG} = 1$  will be retained. For such a trajectory the dependences of the amplitude values of generator voltage and current ( $u_{Go}^*, i_{Go}^*$ ), the power factor ( $\chi_{SG}$ ) and the generated power  $P_{WT0}^* = P_{Ro}^*$  as a function of the frequency of rotation are shown in fig.29. In fig.29a the movement trajectory "«  $a \rightarrow b$  »" occurs in mode 1, in fig.29b, respectively, in mode 2.

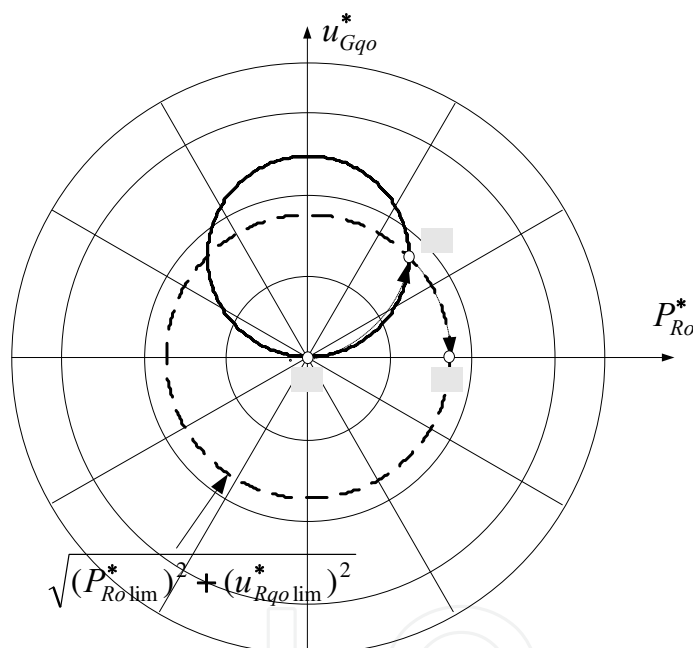


Fig. 28.

As follows from fig.29 at work in the 1st mode, despite the fact that  $\cos \varphi_{SG} = 1$  the power factor of the generator has a little value when  $\omega^* \rightarrow \omega_{WT\min}^*$  it is explained by sufficiently small value of the coefficient of distortion of the generator voltage at low frequencies. In addition, there is a large value of the generator current, so when  $\omega^* \rightarrow \omega_{WT\min}^*$ ,  $i_{Go}^* \rightarrow 1$  i.e. the current is close to the value of short-circuit current. When working in 2nd mode the power factor is much bigger, with the generator current is much smaller than in mode 1. In the 2nd mode, the generator voltage has increased, but it is less than the EMF-load of the generator current.

Note that if we want to save  $\cos \varphi_{SG} = 1$  in the entire working range and  $M \leq 1$  at  $\omega^* = \omega_{WT\max}^*$  as well as to choose the frequency of rotation of WT from the condition

$\omega_{WT\max}^* > \omega_{\max\lim}^*$  the working point of the trajectory at maximum frequency of rotation and maximum power generated will be in the 1st mode (fig.30) and, consequently, will have a low value of power factor.

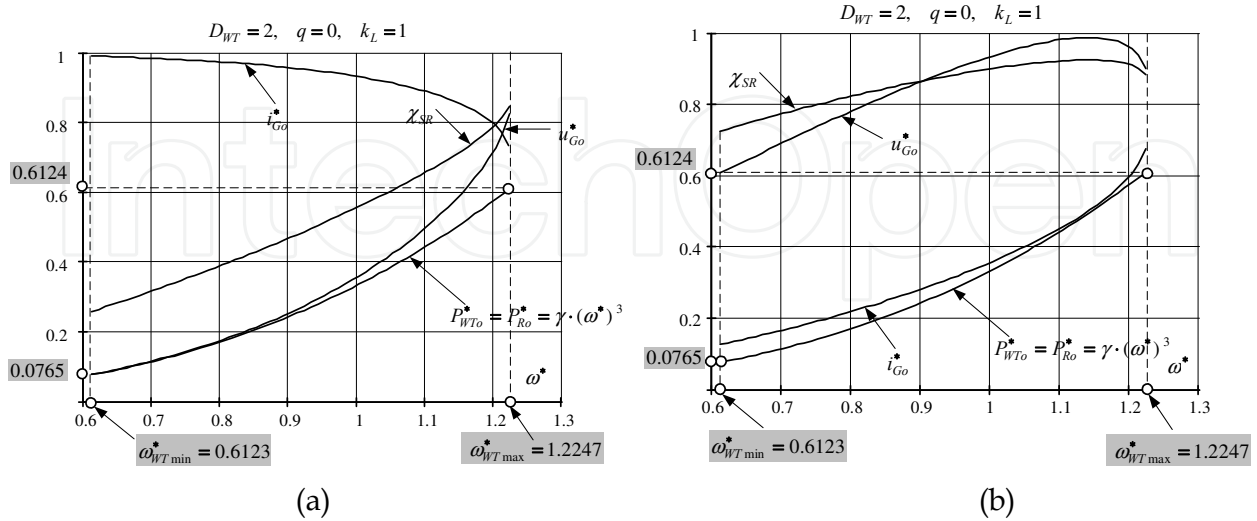


Fig. 29.

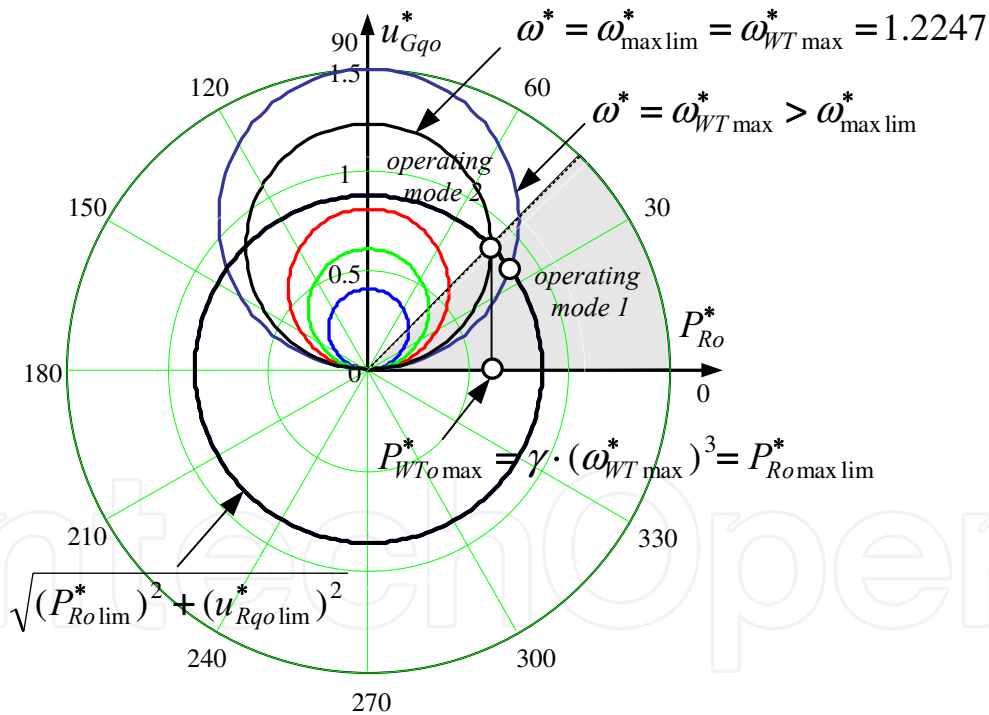


Fig. 30.

Taking into account the results obtained, we can conclude that the work with  $\cos\varphi_{SG} = 1$  in the 1st mode is not optimal for WPGS, because in the entire frequency range  $\omega^* \in \{\omega_{WT\min}^*, \omega_{WT\max}^*\}$  there is a large value of the generator current ( $i_{Go}^* \rightarrow 1$  at  $\omega^* \rightarrow \omega_{WT\min}^*$ ) and a low power factor ( $\chi_{SG}$ ). If condition  $\cos\varphi_{SG} = 1$  remain in the range of frequencies  $\{\omega_{WT\min}^*, \omega_{WT\max}^*\}$  for WPGS should be recommended the second mode, since in this case, the power factor of the generator in the working

frequency range  $\omega_{w\min}^* < \omega^* < \omega_{w\max}^*$  is large enough, with the generator current is much smaller than in the first mode, but there is an increase in generator voltage.

**Phases of the fundamental harmonics of current and voltage of the generator do not coincide.**

In this mode, the angle can be  $0 > \varphi_{SG}$  or  $\varphi_{SG} > 0$ . Vector diagram for the case  $\varphi_{SG} < 0$  is shown in fig. 5. Basic relations for the determination of voltages, currents and power in the system are given in (14) ÷ (26). For these values of the angle  $\varphi_{SG}$ , as in the case of  $\varphi_{SG} = 0$ , the same value of power can be obtained in the two modes, corresponding to different values of the parameter  $M_q$ .

In the general case, when  $q \geq 0, k_L \geq 1$  the active power  $P_{Ro}^*$  is related to  $M_q$  by the relation:

$$\left(\frac{P_{Ro}^* - P_0}{\gamma_P R_{uP}}\right)^2 + \left(\frac{u_{q0}^* - U_0}{R_{uP}}\right)^2 = 1, \tag{45}$$

where

$$\gamma_P = \sqrt{\frac{k_L + q}{1 + q}}; \quad R_{uP} = \frac{\omega^*}{2} \sqrt{1 + \left(\frac{tg\varphi_{SG}}{\gamma_P}\right)^2}; \quad U_0 = \frac{\omega^*}{2}; \quad P_0 = \frac{\omega^*}{2} \frac{tg\varphi_{SG}}{\gamma_P^2}.$$

Whence:

$$u_{q01,2}^* = U_0 \mp \sqrt{(R_{uP})^2 - \left(\frac{P_{Ro}^* - P_0}{\gamma_P}\right)^2}; \quad u_{Ro}^* = \gamma_P^2 P_{Ro}^*; \quad M_{q1,2} = \frac{2}{\sqrt{3}} u_{q01,2}^*; \quad M_d = \frac{2}{\sqrt{3}} \gamma_P^2 P_{Ro}^*.$$

Here the indices "1" and "2" correspond to the 1st and 2d modes in accordance with fig.20. Maximum power achievable at a given frequency of rotation ( $\omega^*$ ) is defined by the relation:

$$P_{Ro\max}^* = P_0 + \gamma_P R_{uP} \equiv \omega^*/2. \tag{46}$$

Relationships (97) make possible to determine the dependence of the currents and voltages in the system as a function of frequency of rotation for different values of the angle  $\varphi_{SG}$  and the parameters  $q$  and  $k_L$ . Major trends of these relationships can be seen on the graphs (22) ÷ (25).

Let us consider the choice of mode of the system in WPI, while we assume that  $q = 0, k_L = 1$ .

In this case, the equation (45) in polar coordinates will be:

$$\begin{aligned} \rho(\phi) &= \omega^* \sec(\varphi_{SG}) \sin(\phi + \varphi_{SG}); \\ P_{Ro}^*(\phi) &= U_{do}^* = \omega^* \sec(\varphi_{SG}) \sin(\phi + \varphi_{SG}) \cos(\phi); \\ u_{q0}^*(\phi) &= \omega^* \sec(\varphi_{SG}) \sin(\phi + \varphi_{SG}) \sin(\phi). \end{aligned} \tag{47}$$

Fig.31 shows the nature of the proposed change of the angle ( $\varphi_{SG}$ ) of current shift ( $i_{G0}^*$ ) on voltage ( $u_{G0}^*$ ) and  $\cos\varphi_{SG}$  on the frequency of rotation of the shaft of WT. The proposed

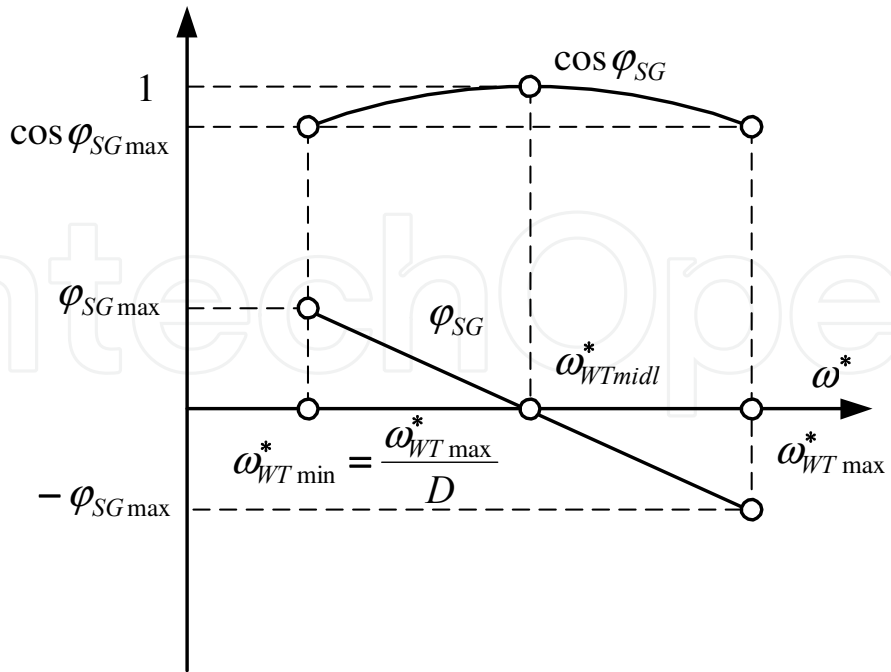


Fig. 31.

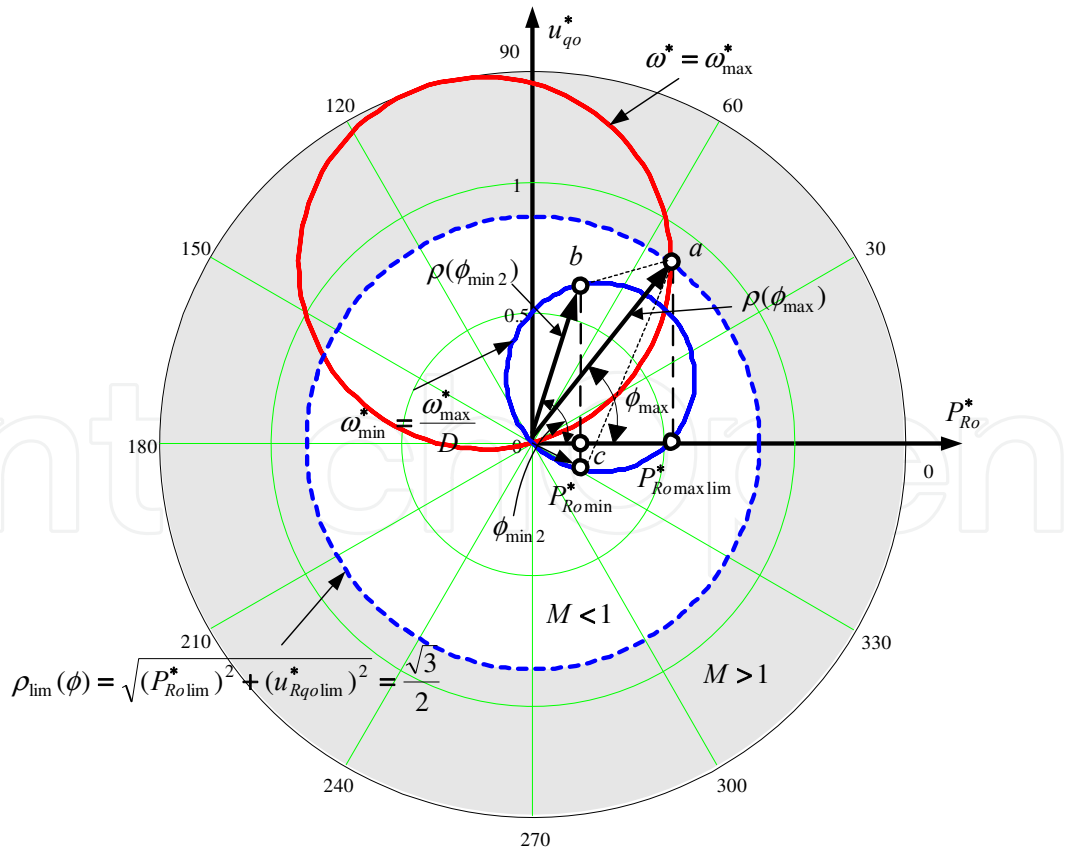


Fig. 32.

scenario allows us to work with  $\omega_{WT\max}^* > \omega_{\max\lim}^*$  remaining in the second mode ( $\omega_{\max\lim}^*$  is defined according to (44)). For this operating point with a maximum power of WT  $P_{WT0\max}^*(\omega_{WT\max}^*)$  is compatible with the maximal achievable power  $P_{Ro\max}^*$  (46), (47). In addition, we require that the power  $P_{Ro\max}^*$  corresponds to  $M=1$  (fig.32), i.e.  $P_{Ro\max}^* = P_{Ro\max\lim}^*$ .

Angle  $\phi_{\max}$  (fig.32) is determined from the equation  $\frac{d\rho(\phi)}{d\phi} = 0$ ,  $\phi_{\max} = \frac{\pi}{4} - \frac{\varphi_{SG}}{2}$ .

We will find the frequency of rotation at which the equality  $P_{Ro\max}^* = P_{Ro\max\lim}^*$  is realized, from the equation:  $\rho(\phi_{\max}) = \sqrt{3}/2$ , it follows that

$$\omega_{\max}^* = \frac{\sqrt{3}}{2} \left[ \sec(\varphi_{SG}) \sin\left(\frac{\pi}{4} + \frac{\varphi_{SG}}{2}\right) \right]^{-1}. \quad (48)$$

Based on (47) ÷ (48)  $P_{Ro\max\lim}^* = \frac{\sqrt{3}}{2} \cos\left(\frac{\pi}{4} - \frac{\varphi_{SG}}{2}\right)$ .

Then we require that

$$\omega_{WT\max}^* = \omega_{\max}^*; \quad P_{WT0\max}^* = P_{Ro\max\lim}^*.$$

Proceeding from the equation (20)  $\gamma = P_{Ro\max\lim}^* / (\omega_{\max}^*)^3$ ,  $P_{WT0}^*(\omega^*) = \gamma(\omega^*)^3$ .

In accordance with fig.31 we take  $\varphi_{SG} = -\varphi_{SG\max}$  when  $\omega^* = \omega_{\max}^*$ . The law of change of  $\varphi_{SG}$  in the operating range  $\omega^* \in \{\omega_{WT\min}^*, \omega_{WT\max}^*\}$  according to fig.31 will look as follows

$$\varphi_{SG}(\omega^*) = \varphi_{SG\max} \left( 1 - 2 \frac{\omega^* - \omega_{\min}^*}{\omega_{\max}^* - \omega_{\min}^*} \right),$$

where  $\omega_{\min}^* = \omega_{WT\min}^* = \omega_{WT\max}^* / D = \omega_{\max}^* / D$ .

Then

$$\omega_{\max}^* = \frac{\sqrt{3}}{2} \left[ \sec(\varphi_{SG}) \sin\left(\frac{\pi}{4} - \frac{\varphi_{SG\max}}{2}\right) \right]^{-1}; \quad P_{Ro\max\lim}^* = \frac{\sqrt{3}}{2} \cos\left(\frac{\pi}{4} + \frac{\varphi_{SG\max}}{2}\right).$$

The minimum power at  $\omega^* = \omega_{WT\min}^*$ :  $P_{Ro\min}^* = P_{Ro\max\lim}^* / D^3$ .

The locus corresponding to the frequency of rotation  $\omega^* = \omega_{WT\min}^*$  is:  $\rho(\phi) = \omega_{WT\min}^* \sec(\varphi_{SG\max}) \sin(\phi + \varphi_{SG\max})$ .

The angle  $\phi = \phi_{\min}$  at  $\omega^* = \omega_{WT\min}^*$  is determined from the equation

$$\begin{aligned} \omega_{WT\min}^* \sec(\varphi_{SG\max}) \sin(\phi_{\min} + \varphi_{SG\max}) \cos \phi_{\min} &= P_{Ro\max\lim}^* / D^3 \\ \phi_{\min 1} &= \frac{1}{2} \arcsin \left[ 2 \frac{P_{Ro\max\lim}^*}{D^2 \omega_{WT\max}^* \sec(\varphi_{SG\max})} - \sin(\varphi_{SG\max}) \right] - \varphi_{SG\max}; \\ \phi_{\min 2} &= \pi/2 - (\phi_{\min 1} + \varphi_{SG\max}). \end{aligned} \quad (49)$$

In the relation (49) angles  $\phi_{\min 1}$  and  $\phi_{\min 2}$  correspond to the 1st and 2d modes.

When the rotation frequency  $\omega_{WT \min}^* \leftrightarrow \omega_{WT \max}^*$  changes the two trajectories are possible (fig.32), namely, «  $a \leftrightarrow c$  » and «  $a \leftrightarrow b$  » with the first corresponding to the system in the 1st mode, and the second - in the 2nd mode.

As already noted, the first mode is characterized by the low value of power factor and the big value of current. For this reason, the second trajectory is desirable, i.e. work in the second mode. In this case:

$$M_d(\omega^*) = 2P_{WT0}^*(\omega^*)/\sqrt{3}; \quad M_q(\omega^*) = \omega^*/2 + \sqrt{(\omega^*/2)^2 - [P_{WT0}^*(\omega^*)]^2 + \omega^* \operatorname{tg}[\varphi_{SG}(\omega^*)]P_{WT0}^*(\omega^*)}.$$

For  $\varphi_{SG \max} = \pi/12$ ,  $D=2$  and  $D=3$  the result of calculation in fig. 33, when  $\omega^* \in \{\omega_{WT \min}^*, \omega_{WT \max}^*\}$ .

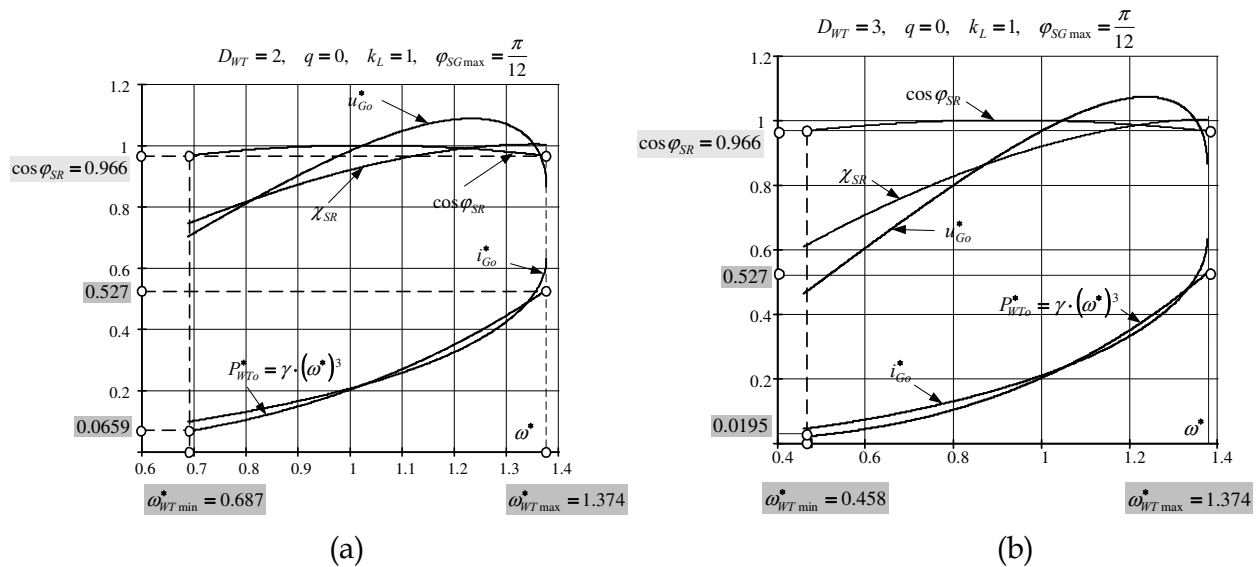


Fig. 33.

As can be seen from the figure 33 that choice of scenario allows a wide range of changes of the frequency of rotation by increasing the value of  $\omega_{\max}^*$  at the given value of  $\cos \varphi_{SG}$ . Dependence of  $\omega_{\max}^*$  on the given value of the angle  $\varphi_{SG \max}$  is presented in fig.34, which implies that the maximum achievable value of the frequency  $\omega_{\max}^*$  for a given scenario of control is equal to  $\sqrt{3}$ .

It should be noted that the selected above the linear law of change of  $\varphi_{SG}(\omega^*)$  is not unique. In that case, if for the area of installing of WPI the prevailing wind speed is known, then the frequency of rotation of the shaft of WT is calculated and at an obtained frequency the point with  $\cos \varphi_{SG} = 1$  is selected. The law of changes the function  $\varphi_{SG}(\omega^*)$  can be optimized according to the change in the winds, with equality  $\cos \varphi_{SG}$  at the extreme points of the operating range  $\{\omega_{WT \min}^*, \omega_{WT \max}^*\}$  is not obligatory.

Thus, the scenario of the WPGS system working according to the given law of change of  $\cos \varphi_{SG}$  with change of  $\omega_{WT}^*$  allows to increase the maximum operating frequency of rotation while maintaining the 2-second mode, which is characterized by relatively high value of power factor.

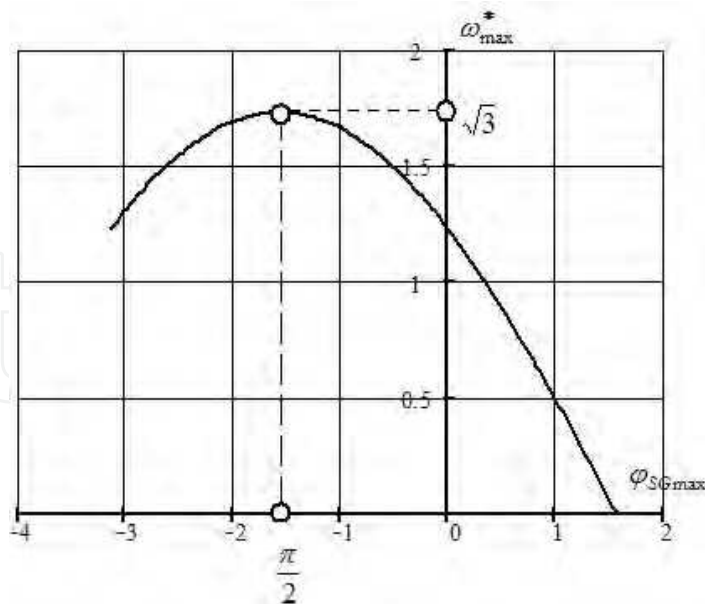


Fig. 34.

#### 4. Basic power indicators in the circuit "voltage inverter - electrical network"

The schematic diagram of the circuit "voltage inverter - electrical network" taking into account the accepted assumptions is shown in fig.35. The estimated mathematical model of the electrical circuit is shown in fig. 4.

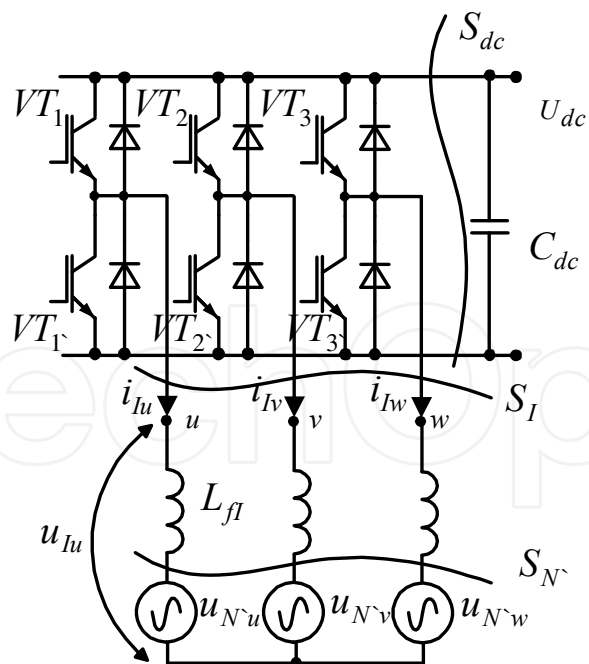


Fig. 35.

Voltage of the electrical network changes according to the law:

$$u_{N^m} = U_N \cdot \cos[v - (m - 1)2\pi/3]; v = \Omega t; m = 1, 2, 3 (u, v, w).$$

Change laws of the inverter control signals are  $u_{lcm} = u_c \cos(\theta_m)$ , where  $\theta_m = \nu - (m-1)2\pi/3 + \varphi_{lc}$ ;

Taking into account the accepted assumptions the mathematical model of an electric circuit in rotating system of coordinates, under condition of orientation on an axis of voltage of an electric network  $q$ , will look like:

$$\mathbf{u}_I - \mathbf{u}_{N^*} = \mathbf{r}_I \mathbf{i}_I + L_I \frac{d}{dt} \mathbf{i}_I + L_I \boldsymbol{\Omega} \cdot \mathbf{i}_I, \quad (50)$$

where:  $\mathbf{u}_I = [u_{Id} \quad u_{Iq}]^t$ ,  $\mathbf{u}_{N^*} = [0 \quad U_{N^*}]^t$ ,  $\mathbf{i}_I = [i_{Id} \quad i_{Iq}]^t$  - vectors of the inverter voltage and the mains voltage, vector of the inverter currents;  $U_{N^*}$  - the peak value of network voltage;  $\mathbf{r}_I = \text{diag}\{r_I, r_I\}$ ,  $r_I$  - the resistance of inductance of power filter and of the transformer windings;  $L_I$  - the equivalent inductance of the power filter and the transformer leakage inductance;  $\boldsymbol{\Omega} = \begin{bmatrix} 0 & -\Omega \\ \Omega & 0 \end{bmatrix}$ ,  $\Omega$  - circular frequency of the network voltage.

Neglecting the active resistance the ratio (50) can be written in a scalar form

$$u_{Id} \approx L_I \frac{di_{Id}}{dt} - \Omega \cdot L_I i_{Iq}, \quad u_{Iq} - U_{N^*} \approx L_I \frac{di_{Iq}}{dt} + \Omega \cdot L_I i_{Id}. \quad (51)$$

A mathematical model of the inverter will be determined by the relations (5) ÷ (8). In these relationships we take:  $U_{dc} = \sqrt{3} \cdot U_{N^*} \cdot \delta_{Udc}$ , where  $\sqrt{3} \cdot U_{N^*}$  - is the minimal possible voltage in a direct current link with SPWM,  $\delta_{Udc}$  - is excess of the minimal possible voltage of a link of a direct current.

As before, in order to preserve the universality of the results of the analysis, we introduce the following relative units:  $E_{\bar{\sigma}} = U_{N^*}$ ;  $\omega_{\bar{\sigma}} = \Omega$ ;  $X_{\bar{\sigma}} = \omega_{\bar{\sigma}} L_I$ ;  $I_{\bar{\sigma}} = I_{\kappa 3} = E_{\bar{\sigma}} / X_{\bar{\sigma}}$ ;  $S_{\bar{\sigma}} = 3E_{\bar{\sigma}} I_{\bar{\sigma}} / 2$ ;  $a_I = \omega_{cl} / \Omega$ ; where  $\omega_{cl}$  - a cyclic frequency of the PWM inverter.

Taking into account relative units the equation (51) will become:

$$u_{Id}^* = \frac{di_{Id}^*}{dv} - i_{Iq}^*, \quad u_{Iq}^* - 1 = \frac{di_{Iq}^*}{dv} + i_{Id}^*,$$

where  $\nu = \Omega t$ .

The voltages  $u_{Id}^*$  and  $u_{Iq}^*$  are determined by the relations

$$u_{Id}^* = u_{Ido}^* + \Delta u_{Id}^*; \quad u_{Iq}^* = u_{Iqo}^* + \Delta u_{Iq}^*;$$

$$u_{Ido}^* = \frac{\sqrt{3}}{2} \delta_{Udc} M \sin(-\varphi_{Rc}) = -\frac{\sqrt{3}}{2} \delta_{Udc} M_d; \quad u_{Iqo}^* = \frac{\sqrt{3}}{2} \delta_{Udc} M \cos(-\varphi_{Rc}) = \frac{\sqrt{3}}{2} \delta_{Udc} M_q;$$

here  $u_{Ido}^*$ ,  $u_{Iqo}^*$  - the orthogonal components in the  $d$  and  $q$  coordinates of the fundamental harmonic of inverter voltage;  $\Delta u_{Id}^*$ ,  $\Delta u_{Iq}^*$  - the orthogonal components in the  $d$  and  $q$  coordinates of the high-frequency harmonics of inverter voltage.

We will define the high-frequency harmonics for SPWM from the relations (14).

The equation for the inverter current can be represented as the sum of the fundamental ( $i_{Ido}^*$ ,  $i_{Iqo}^*$ ) and the high frequency ( $\Delta i_{Id}^*$ ,  $\Delta i_{Iq}^*$ ) harmonics  $i_{Id}^* = i_{Ido}^* + \Delta i_{Id}^*$ ;  $i_{Iq}^* = i_{Iqo}^* + \Delta i_{Iq}^*$ . The fundamental harmonic of the inverter current is determined by the relation

$$i_{Iqo}^* = -u_{Ido}^*; \quad i_{Id}^* = u_{Iqo}^* - 1.$$

The high-frequency harmonics of the inverter current for SPWM are determined from the relations (16).

We assume such a control law of inverter, when the WPI in electrical circuit generates only an active power. Then the vector diagram for the fundamental harmonic of current and voltage will have the form shown in fig.36.

Under such a control  $u_{Iqo}^* = 1$ ;  $i_{Io}^* = i_{Iqo}^* = -u_{Ido}^*$ ;  $i_{Id}^* = 0$ . Generated in the electrical network active power is:

$$P_{No}^* = i_{Iqo}^* = i_{Io}^* = -u_{Ido}^*. \tag{52}$$

Vector diagram for the orthogonal components ( $M_d, M_q$ ) of the inverter control signal in « $d$   $q$ » coordinates is presented in fig.37

The quantities  $M_d, M_q$  and  $\varphi_{Ic}$  are determined by the relations:

$$M_q = 2 / (\sqrt{3}\delta_{Udc}), \quad M_d = 2P_{No}^* / (\sqrt{3}\delta_{Udc}), \quad \varphi_{Ic} = \arctg M_d / M_q = \arctg P_{SNo}^*. \tag{53}$$

The linear range of work of the inverter is limited by a condition:

$$\sqrt{(M_d)^2 + (M_q)^2} \leq \begin{cases} 1 - SPWM; \\ \frac{2}{\sqrt{3}} - SVPWM. \end{cases}$$

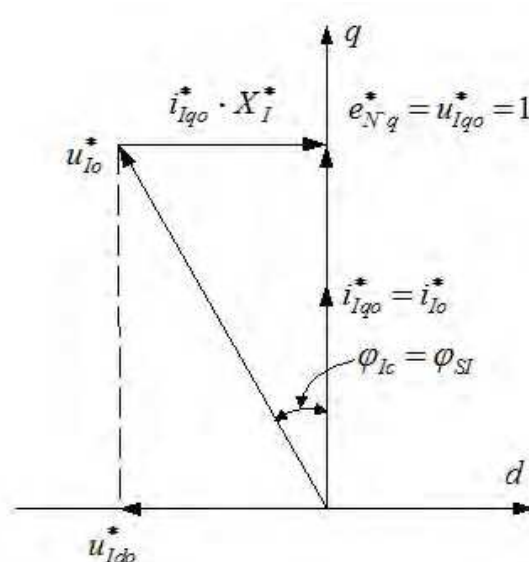


Fig. 36.

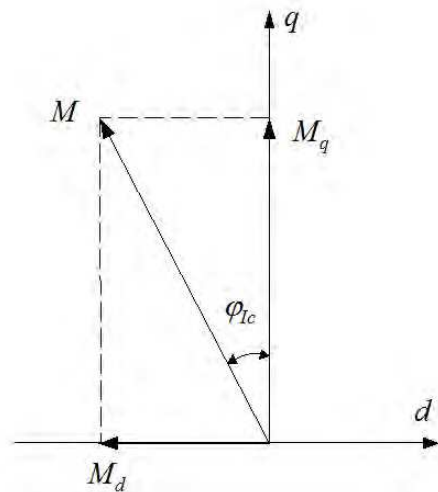


Fig. 37.

From (53) (in the case of equality), we obtain an expression for the maximum active power ( $P_{No\max}^*$ ), which can be transferred to the electricity grid without distortion of the current.

$$P_{No\max}^* = \begin{cases} \sqrt{\left(\frac{\sqrt{3}}{2} \delta_{Udc}\right)^2 - 1}, & \text{1SPWM} \\ \sqrt{(\delta_{Udc})^2 - 1}, & \text{-SVPWM.} \end{cases}$$

The dependence of  $P_{No\max}^*$  on the value of  $\delta_{Udc}$  is shown in fig.38, which implies that the minimum value of  $\delta_{Udc\min}$  at which the generation of active power begins is given by:

$$\delta_{Udc\min} = \begin{cases} \frac{2}{\sqrt{3}} & \text{-SPWM;} \\ 1 & \text{-SVPWM.} \end{cases}$$

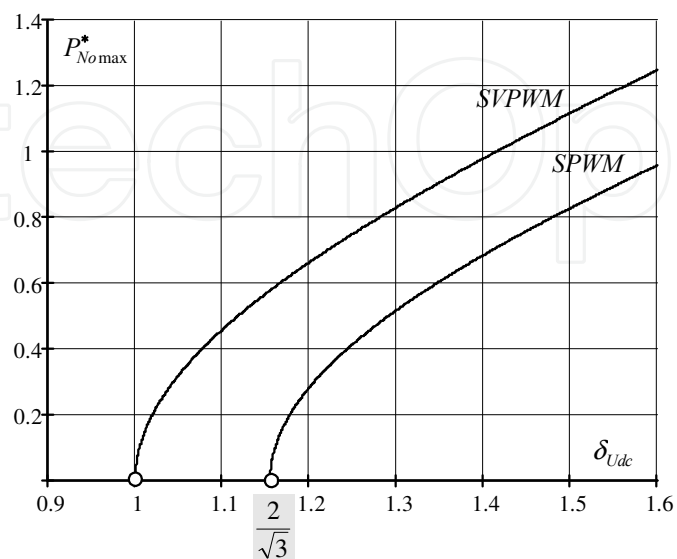


Fig. 38.

Dependence of the active power  $P_{No}^*$  from the relative values of voltage in the DC link  $\delta_{Udc} = U_{dc} / \sqrt{3}U_N$ , and the depth (index) of modulation  $M$  can be found from the following relation:

$$P_{No}^* = \sqrt{(\sqrt{3}\delta_{Udc}M / 2)^2 - 1} . \tag{54}$$

Taking into account the active losses in the output circuit of the generating system an expression for the fundamental harmonic current and the active power will look like

$$i_{lo}^* = P_{No}^* = \frac{1}{1 + (\omega_R^*)^2} \cdot \left\{ -\omega_R^* + \sqrt{[1 + (\omega_R^*)^2] \left( \frac{2}{\sqrt{3}\delta_{Udc}M} \right)^2 - 1} \right\};$$

where  $\omega_R^* = R/X_\sigma$ ,  $R$  - the equivalent active resistance of the inverter phase.

Graph of this dependence (at  $\omega_R^* = 0$ ) for SPWM and SVPWM is shown in fig.39, which implies that the adjustment range of active power decreases with decreasing of  $\delta_{Udc}$ . It should be noted that when working on electrical network application of SVPWM can significantly increase the active power. As follows from fig.40 for each the value of  $\delta_{Udc}$  there is a minimum value of modulation depth  $M_{min}$  below which the generating active power is equal to zero  $M_{min} = 2/(\sqrt{3}\delta_{Udc})$ .

The dependence of  $M_{min}$  on  $\delta_{Udc}$  is shown in fig.40.

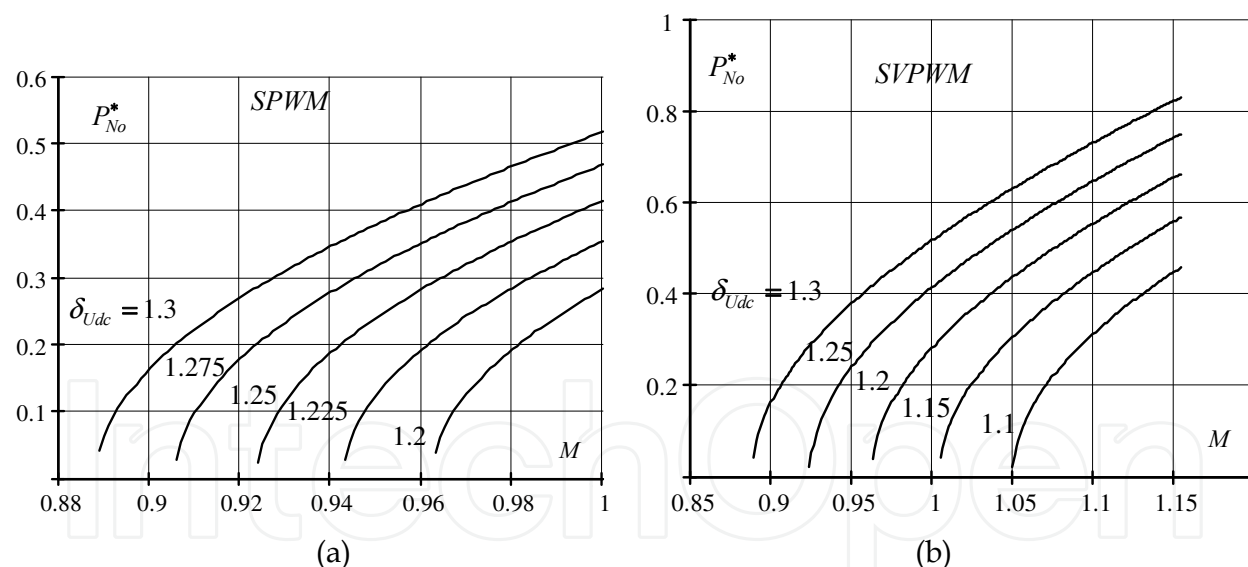


Fig. 39.

We determine how vary the coefficients of harmonics ( $THD_{il}$ ) and distortions ( $v_{il}$ ) of the inverter current. In accordance with the relations (52) and (19) the effective value of the fundamental harmonic of inverter current ( $i_{lo,rms}^*$ ), its fluctuating components ( $\Delta i_{l,rms}^*$ ) and the total effective value ( $i_{l,rms}^*$ ) are defined as follows:

$$i_{lo,rms}^* = P_{No}^* / \sqrt{2}, \Delta i_{l,rms}^* = \left( \frac{\sqrt{3}\delta_{Udc}}{\pi \cdot X_\Sigma^*} \right) \cdot \left( J_1(\pi \cdot M)^2 \frac{a_l^2 + 1}{(a_l + 1)^2 (a_l - 1)^2} \right)^{\frac{1}{2}}, i_{l,rms}^* = \sqrt{(i_{lo,rms}^*)^2 + (\Delta i_{l,rms}^*)^2} \tag{55}$$

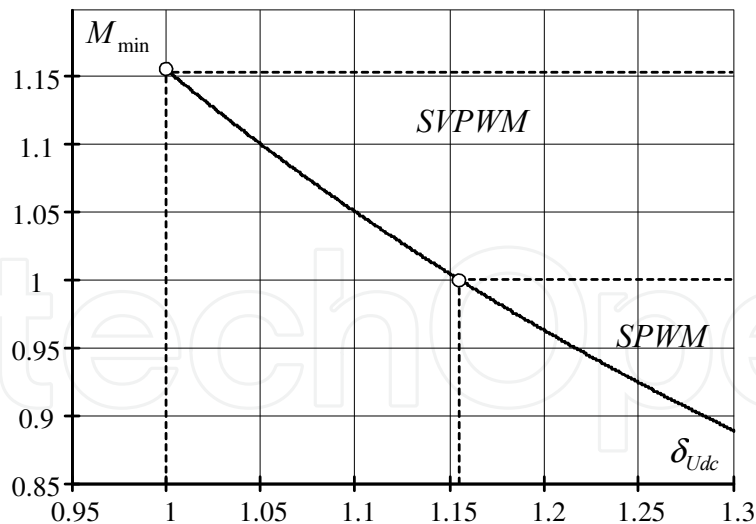


Fig. 40.

In fig.41 the dependence of the magnitudes  $THD_{il}$  and  $v_{il}$  as a function of the depth of modulation  $M$  with  $\delta_{Udc} = 1.3$  is presented. As follows from this figure, the qualitative indicators of a current are much worse with a decrease in modulation depth, while the value  $THD_{il} = 0.05$  is reached at  $M \rightarrow 1$  and  $\delta_{Udc} \geq 1.3$ . For the Russian standards, the quality of the generated electric current in the WPI network must fulfill the condition  $THD_{il} \leq 0.05$ . It should also be noted that  $THD_{il}$  practically does not depend on the inductance  $L_l$  and is determined only by the multiplicity of frequencies  $a_l$  and the ratio of voltages  $\delta_{Udc}$ .

Taking into account that the phase of the inverter current coincides with the phase of voltage of the electrical network, as well as a sinusoidal change of the voltage, taking into account the relations (13) we obtain the following expression for the power factor in the cross section  $S_N$ :  $\chi_N = P_{No}^* / S_N^* = v_{il}$ .

We define the changes in  $THD_{il}$  and  $v_{il}$  in the WPI, as function of the frequency of rotation of the shaft of WT. We assume

$$P_{WT0}^* = \gamma \cdot (\omega / \omega_{WTmax})^3. \quad (56)$$

We define the coefficient  $\gamma$  according to the condition  $P_{WT0}^*(\omega_{WTmax}) = P_{No}^*$ , then  $\gamma = P_{No}^*$ . Based on the (54) and (56) we obtain the dependence of modulation depth on the frequency of rotation of the shaft of WT

$$M = \frac{2}{\sqrt{3}\delta_{Udc}} \sqrt{\left[ P_{No}^* \cdot \left( \frac{\omega}{\omega_{WTmax}} \right)^3 \right]^2 + 1}. \quad (57)$$

In fig.42 the dependence of  $M$  on  $\omega / \omega_{WTmax}$  for the two types of modulation (SPWM and SVPWM) is presented. It implies that the modulation depth varies slightly.

Knowing the dependence of  $M$  on  $\omega / \omega_{WTmax}$ , we can determine the changes of the qualitative characteristics of the generated energy as the function of the frequency of rotation of the shaft of WT. For this we use the relations (55) (57).

In fig.43 graphs of  $THD_{il}$  and  $v_{il}$  on  $\omega / \omega_{WTmax}$  for SPWM are presented.

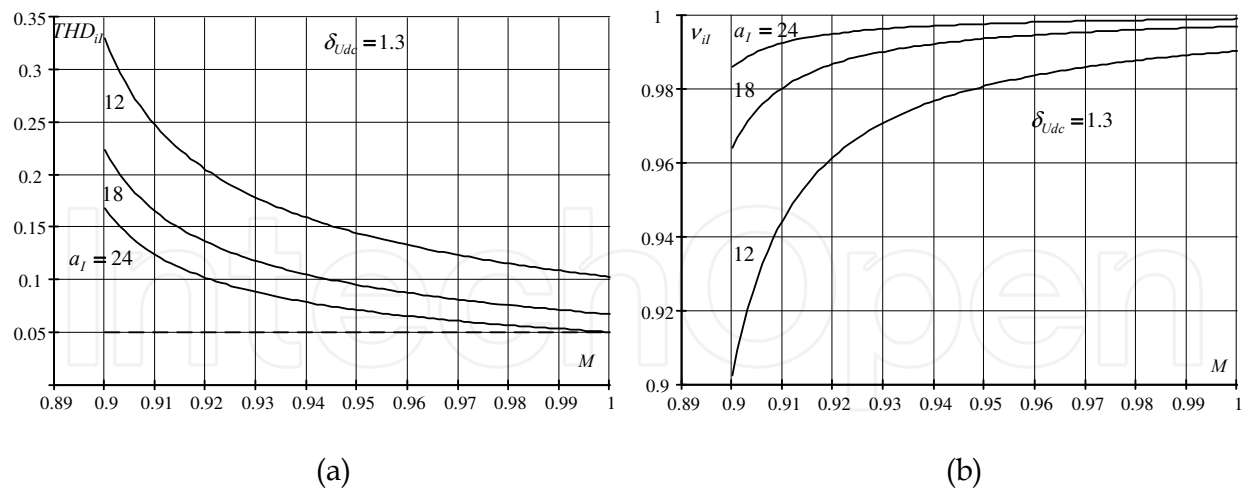


Fig. 41.

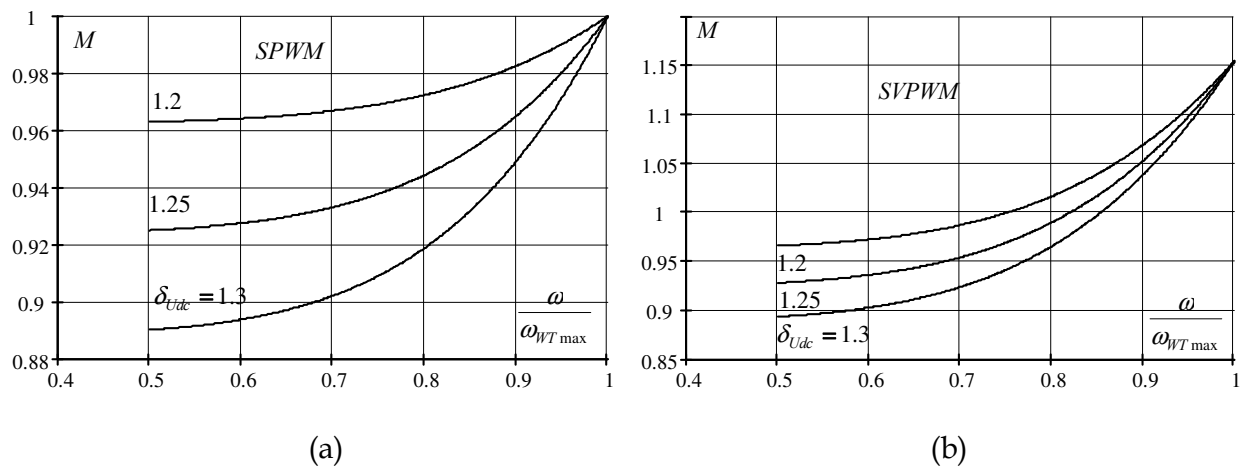


Fig. 42.

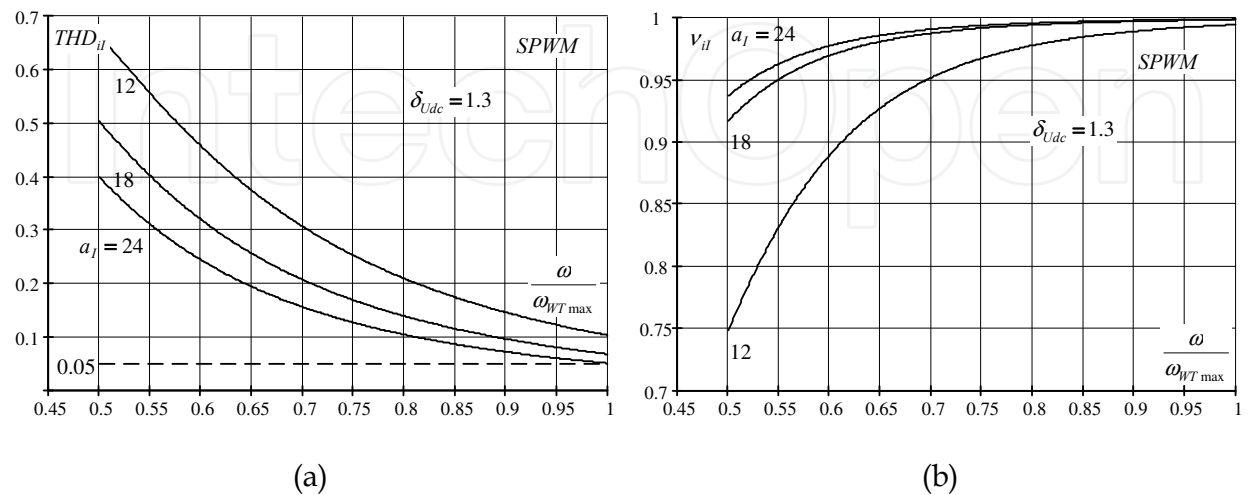


Fig. 43.

Given that in the powerful WPI multiplicity of frequencies  $a_l$  is limited by the dynamic losses in the semiconductor switches, we can conclude that it is impossible to satisfy the requirements of the quality of the generated energy by increasing the PWM frequency, as in the case of SPWM, and when SVPWM.

There is a positive impact of increase in the parameter  $\delta_{Udc}$  on the quality of electric power, but it leads to a significant increase in the DC link voltage and, consequently, to increase of the installed capacity of the electric power converter.

The solution of this problem can be modification of the voltage inverter circuit or reducing the range of power change implementing SVPWM.

When constructing the WPI of MW capacity and more one should be guided by the multilevel inverter circuits.

However, one of the ways of solving the problem may be the shunting "m" inverters connected to a DC voltage source controlled by the same modulating signal at the output of each phase, but the time of entry gates are shifted relative to each other in frequency  $\omega$  and at an angle  $2\pi/m$  that is carried out, for example, in bilateral sinusoidal PWM introducing of m sources of reference signals with a specified phase shift. This decision, in addition to improving the quality of energy, increases its level, providing a modular inverter and system as a whole. The modular principle of the considered WPGS also has the advantage that it can save about the same level of efficiency of large and small rotational velocities, which provided by the different numbers of modules in the function of the frequency of rotation of the shaft of the wind turbine. Fig.44 shows an example of parallel connection of m inverters.

In parallel connection, each inverter independently from the other forms voltage  $u_{li}$ , which value can be determined in accordance with the relation (6). This parallel connection is possible if the parallel channels have no common inductance, i.e. each channel operates on the electrical network, or at the entrance of a transformer there is a capacitive filter on which high-frequency ripple voltage is practically equal to zero.

Each of the phases of such a system can be represented as an equivalent circuit (fig.45). For this scheme the following relations are fair

$$i_l = \sum_{i=1}^m i_{li}, \quad u_{el} = \frac{1}{m} \sum_{i=1}^m u_{li}; \quad L_{le} = \frac{L_l}{m}, \quad i_{dc} = \sum_{i=1}^m i_{dci},$$

where  $u_{el}$ ,  $L_{le}$  - the equivalent internal voltage and inductance.

The total generated power of the system of m channels will be determined by the ratio  $P_{N'o} = \sum_{i=1}^m P_{N'oi}$ , where  $P_{N'oi}$  - the active power of the i-th channel.

Fig.46 shows an example [2] of calculated the equivalent inverter voltage waveform ( $u_{le}$ ) and locus of voltage  $u_{ldq}^*$  at  $m=3$ . Locus structure is similar to the equivalent multi-level inverter. This conclusion is illustrated by the amplitude-frequency spectrum of the current  $i_l$  given at fig.47 for the three options  $m=1,3$  (at  $a_l=20$ ).

Increase in the number of channels leads to exclusion from the spectrum of the current of groups of combinational harmonics with frequencies  $\nu = n \cdot \omega_{kl} \pm p \cdot \Omega$ ;  $n < m$ .

Calculations show that a reduction in the harmonics of load current  $THD_{i_{l(m)}}$  when you turn on  $m$  parallel channels can be estimated by the ratio  $THD_{i_{l(m)}} = THD_{i_{l(1)}}/m^2$ , where  $THD_{i_{l(1)}}$  - the coefficient of harmonics with  $m = 1$ .

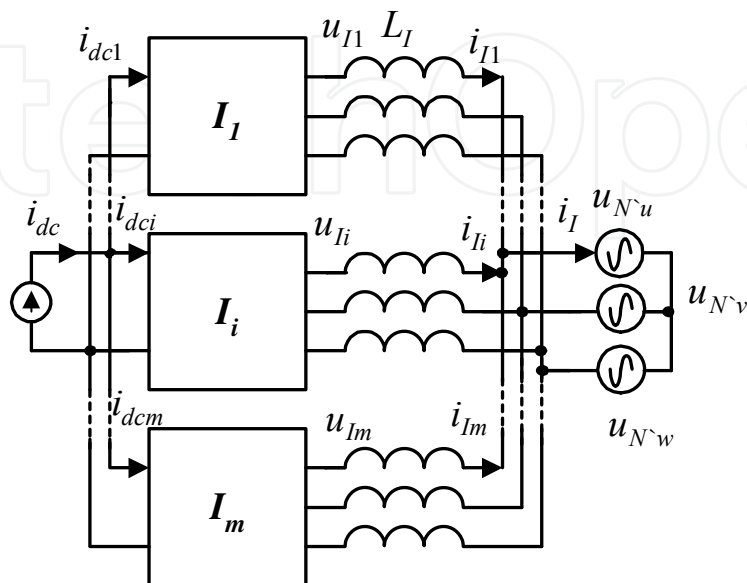


Fig. 44.

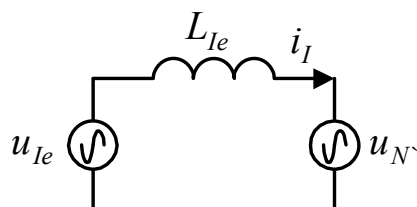


Fig. 45.

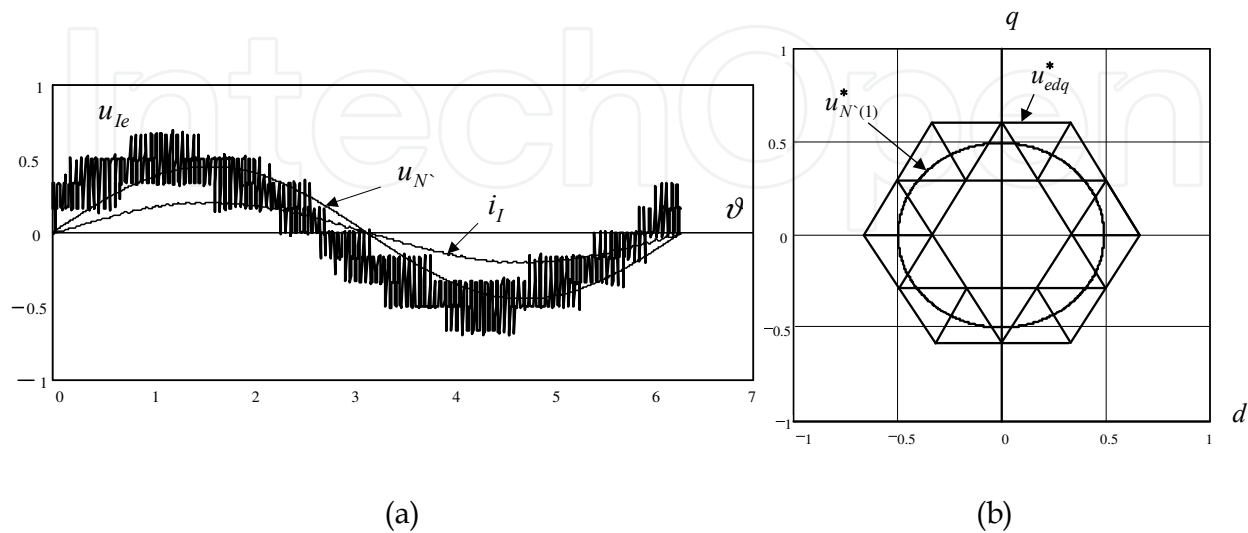


Fig. 46.

Not identical distribution of the active power between the “two neighboring” channels can be evaluated using the following relation

$$\delta_{PN} = \frac{P_{No(i)}^* - P_{No(i+1)}^*}{P_{No(i)}^* + P_{No(i+1)}^*} * 100\% \approx \frac{1}{4} \left( \frac{\pi}{m \cdot a_I} \right)^2 100\% .$$

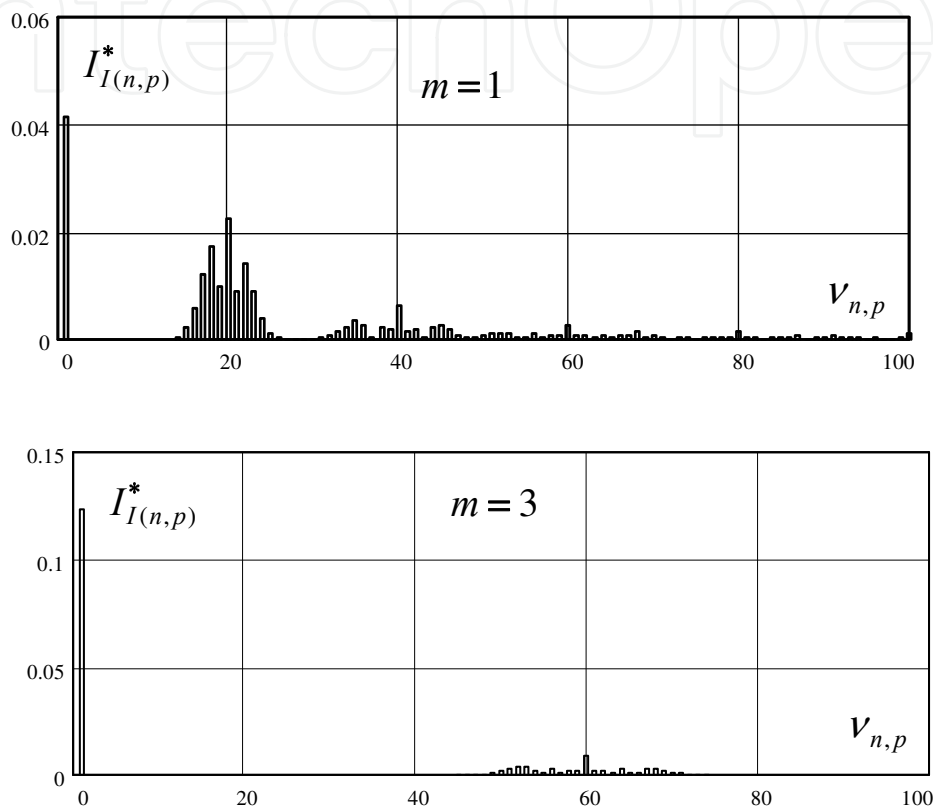


Fig. 47.

The dependence of  $\delta_{PN}$  on the multiplicity of frequencies for different  $m$  is shown in fig.48, which implies that when  $a_I < 8$  and  $m = 2$ , imprecision in the distribution of active power does not exceed one percent. With the increasing  $m$  the error decreases.

Thus, with the reasonable accuracy it can be assumed that

$$P_{No(1)}^* = \dots = P_{No(i)}^* = \dots = P_{No(m)}^*, \quad P_{No}^* = \sum_{i=1}^m P_{No(i)}^* .$$

The analysis shows that the parallel connection of the channels leads to a decrease in the number of groups of combination harmonics in the amplitude-frequency spectrum  $i_{dc}$ , the amplitude of high-frequency harmonics decreases. The power factor ( $\chi_{Sdc(m)}$ ) and the inactive power ( $Q_{Sdc}$ ) in the section  $S_{dc}$  at the voltage inverter input (fig.44) subject to  $m$  parallel channels can be estimated using the relations of the form [2]:

$$\chi_{Sdc(m)} = \frac{P_{No}}{\sqrt{(P_{No})^2 + (Q_{Sdc})^2}} \approx \left[ \sqrt{1 + \frac{1 - (\chi_{Sdc(1)})^2}{(\chi_{Sdc(1)})^2} \cdot \frac{1}{(m)^2}} \right]^{-1}, Q_{Sdc} = P_{No} \cdot \sqrt{1/(\chi_{Sdc(m)})^2 - 1}, (58)$$

where  $\chi_{Sdc(1)}, \chi_{Sdc(m)}$  - power ratios in the cross section  $S_{dc}$  of one channel and  $m$  channels respectively.

From (58) we can conclude that an increase in the number of parallel channels included in the input power increases the component of active power and virtually unchanged a reactive power. Thus, the parallel connection of  $m$  channels leads to an increase in the power generated by  $m$  times, to a decrease of ratio of harmonics of the generated current by factor of about  $m^2$  while maintaining the multiplicity of frequencies  $a_l$ , the specific reactive power of capacitor ( $C_f$ ) in the chain of dc decreases by  $m$  times. When we save the value of the coefficient of harmonics of generated current the shunting channels can reduce the multiplicity of frequencies  $a_l$  by approximately  $m^2$  times.

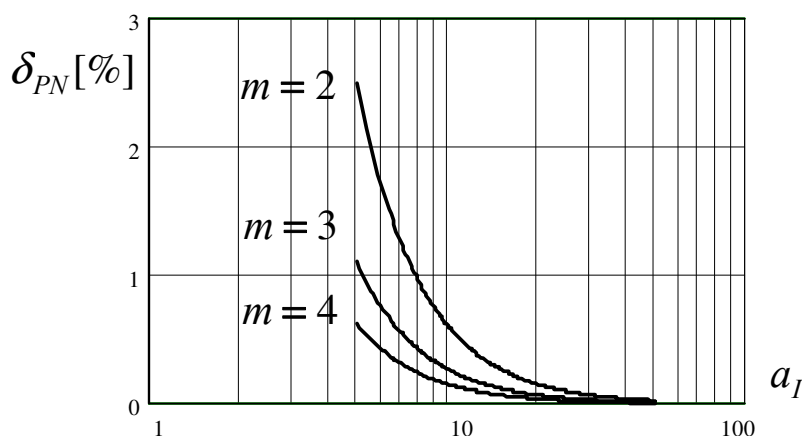


Fig. 48.

Thus, the analysis of energy data in the circuit "voltage inverter - electrical network" provides an opportunity for an analytical assessment of the main parameters and detects trends in integrated settings, and characteristics when changing operating modes and control algorithms. When using the voltage inverter of WPI on the electrical network of the power quality of output current varies considerably. So, for example, at a range of change of frequency of rotation of a shaft of the wind turbine  $D \geq 2$  it is practically impossible to provide at real parameters  $THD_{il} \leq 0.05$  of the power scheme of the inverter in all range of frequencies of rotation. This problem is solved by using SVPWM, multi-level converter circuit, or using the modular principle of the converter. The modular construction principle allows increasing the efficiency of WPGS at low frequencies by turning off the multiple channels. This solution allows extending the working range of wind speeds of WPI. The principle of modular converter can be extended to WPGS; in this case the generation system is constructed, as shown in fig.49. Here, as an example, a system of 4-channel generation is presented. Fig.50 shows the change in power in one channel to generate at different ranges of speed of shaft of WT. It would start one channel, then two, three and four. Increase in the number of working modules reduces the current range of each module, which increases the efficiency of the system at low wind speeds; this increases the maximum capacity of the system, generated by maintaining its high quality. According to this principle the WPI «Raduga-1A» 1 MW was designed and built near Elista.

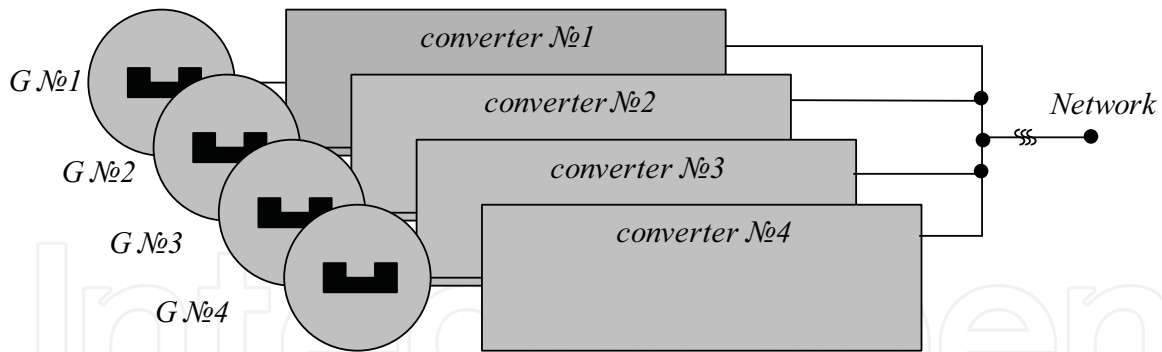


Fig. 49.

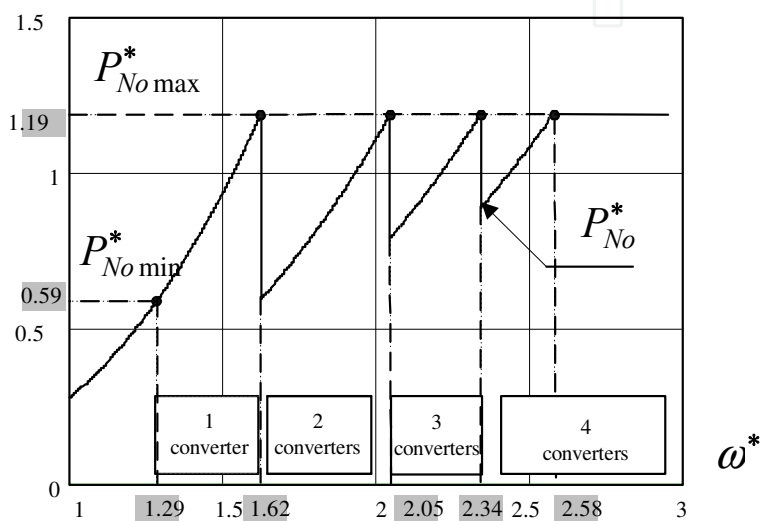


Fig. 50.

## 5. Conclusions

1. A mathematical model for analysis of energy characteristics of electric power generation system consisting of a synchronous generator with excitation from permanent magnets, the active rectifier and the voltage inverter with PWM is considered.
2. Various algorithms to control the active rectifier and inverter for variable speed wind turbine shaft are analyzed.
3. Analytical relations for the calculation of currents, voltages and power generation in the system are obtained.
4. Recommendations on the choice of control algorithms and structural circuits of the generation electrical energy at a variable speed shaft WT are given.

## 6. References

- [1] Corn G., Corn T. Mathematics handbook (for science officers and engineers). - M. - the Science, 1974. in Russian
- [2] Kharitonov S. A. Integrated parameters and characteristics of voltage inverters in structure of generating systems of an alternating current such as "variable speed - constant frequency" for wind-energetic installations / Scientific bulletin NSTU, Novosibirsk, 1999. 92-120 p., in Russian.



## **Wind Power**

Edited by S M Muyeen

ISBN 978-953-7619-81-7

Hard cover, 558 pages

**Publisher** InTech

**Published online** 01, June, 2010

**Published in print edition** June, 2010

This book is the result of inspirations and contributions from many researchers of different fields. A wide variety of research results are merged together to make this book useful for students and researchers who will take contribution for further development of the existing technology. I hope you will enjoy the book, so that my effort to bringing it together for you will be successful. In my capacity, as the Editor of this book, I would like to thank and appreciate the chapter authors, who ensured the quality of the material as well as submitting their best works. Most of the results presented in the book have already been published on international journals and appreciated in many international conferences.

### **How to reference**

In order to correctly reference this scholarly work, feel free to copy and paste the following:

Sergey A. Kharitonov (2010). An Analytical Analysis of a Wind Power Generation System Including Synchronous Generator with Permanent Magnets, Active Rectifier and Voltage Source Inverter, Wind Power, S M Muyeen (Ed.), ISBN: 978-953-7619-81-7, InTech, Available from: <http://www.intechopen.com/books/wind-power/an-analytical-analysis-of-a-wind-power-generation-system-including-synchronous-generator-with-perman>

**INTECH**  
open science | open minds

### **InTech Europe**

University Campus STeP Ri  
Slavka Krautzeka 83/A  
51000 Rijeka, Croatia  
Phone: +385 (51) 770 447  
Fax: +385 (51) 686 166  
[www.intechopen.com](http://www.intechopen.com)

### **InTech China**

Unit 405, Office Block, Hotel Equatorial Shanghai  
No.65, Yan An Road (West), Shanghai, 200040, China  
中国上海市延安西路65号上海国际贵都大饭店办公楼405单元  
Phone: +86-21-62489820  
Fax: +86-21-62489821

© 2010 The Author(s). Licensee IntechOpen. This chapter is distributed under the terms of the [Creative Commons Attribution-NonCommercial-ShareAlike-3.0 License](#), which permits use, distribution and reproduction for non-commercial purposes, provided the original is properly cited and derivative works building on this content are distributed under the same license.

IntechOpen

IntechOpen